

Zeitschrift: IABSE reports = Rapports AIPC = IVBH Berichte
Band: 999 (1997)

Rubrik: Connection between materials

Nutzungsbedingungen

Die ETH-Bibliothek ist die Anbieterin der digitalisierten Zeitschriften auf E-Periodica. Sie besitzt keine Urheberrechte an den Zeitschriften und ist nicht verantwortlich für deren Inhalte. Die Rechte liegen in der Regel bei den Herausgebern beziehungsweise den externen Rechteinhabern. Das Veröffentlichen von Bildern in Print- und Online-Publikationen sowie auf Social Media-Kanälen oder Webseiten ist nur mit vorheriger Genehmigung der Rechteinhaber erlaubt. [Mehr erfahren](#)

Conditions d'utilisation

L'ETH Library est le fournisseur des revues numérisées. Elle ne détient aucun droit d'auteur sur les revues et n'est pas responsable de leur contenu. En règle générale, les droits sont détenus par les éditeurs ou les détenteurs de droits externes. La reproduction d'images dans des publications imprimées ou en ligne ainsi que sur des canaux de médias sociaux ou des sites web n'est autorisée qu'avec l'accord préalable des détenteurs des droits. [En savoir plus](#)

Terms of use

The ETH Library is the provider of the digitised journals. It does not own any copyrights to the journals and is not responsible for their content. The rights usually lie with the publishers or the external rights holders. Publishing images in print and online publications, as well as on social media channels or websites, is only permitted with the prior consent of the rights holders. [Find out more](#)

Download PDF: 19.01.2026

ETH-Bibliothek Zürich, E-Periodica, <https://www.e-periodica.ch>

Composite Construction in Cable-Stayed Bridge Towers

Miguel A. Astiz, born 1950, studied civil engineering at Polytechnical University of Madrid (UPM) and at Stanford University. He is professor of structural engineering and, with Carlos Fernandez Casado S.L., he has been involved in the design and analysis of several long span bridges.

Miguel A. ASTIZ

Professor Dr.

Carlos Fernandez Casado S.L.

Madrid, Spain



Miguel A. Astiz, born 1950, studied civil engineering at Polytechnical University of Madrid (UPM) and at Stanford University. He is professor of structural engineering and, with Carlos Fernandez Casado S.L., he has been involved in the design and analysis of several long span bridges.

Summary

This paper presents an application of composite construction to solve the problem of anchoring the cables to concrete towers in cable-stayed bridges. The use of steel saddles made out of perforated plates is proposed as a compact, economical and fatigue resistant solution to this problem. Design and analysis of such a solution is presented as applied to a cable-stayed bridge with a 203 m long central span.

1. **Introduction**

A well known design problem in cable-stayed bridges consists in anchoring the cables in the tower. As concrete towers are usually the most economic alternative to transmit predominantly axial compression loads to the foundations, many problems arise to transmit horizontal cable force components from front stays to backstays. Moreover, in moderate spans it is difficult to fit both anchorages inside the tower. Several solutions have been proposed to this problem [1,2] although many of them are not fully satisfactory.

Basically the available alternatives consist either in overlapping anchorages (which may lead to awkward arrangements of tubes, anchorages and cables) or designing an internal gallery inside the tower (which means complicated prestressing arrangements as well as important dimensional constraints both for the size of the tower and to manage the jacks) or, finally, anchoring the cables in steel elements which may adopt very different shapes and sizes [2-5].

The solution which is presented here consists in the use of steel saddles which are embedded in tower concrete and which support both anchorages. Adherence between the saddles and concrete is obtained by means of perforated plates. This solution allows a very slender design of the towers as well as a quick positionning of the saddles (thus avoiding usually lengthy positionning of stay tubes).

The design of the saddles has to take into account both their intrinsic resisting properties and the force transmission to concrete. The rationale of the design as well as the analysis of such elements is presented in this paper to show that this is a very valuable alternative for anchoring cable stays in concrete towers.

2. Tower concept

The project for which we have developed this saddle concept is the Papaloapan bridge (Mexico), which was opened for traffic in 1995. This is a cable-stayed bridge with concrete deck and a 203 m long main span (Fig. 1). Because of the very flat landscape, the overall design concept was aimed at minimizing the transverse dimensions of all the elements of the bridge; the depth of the deck is only 1.44 m for 23.4 m width in order to raise the bridge profile as little as possible to reduce the approach embankments. The stays are arranged in two vertical planes, on both sides of the deck.

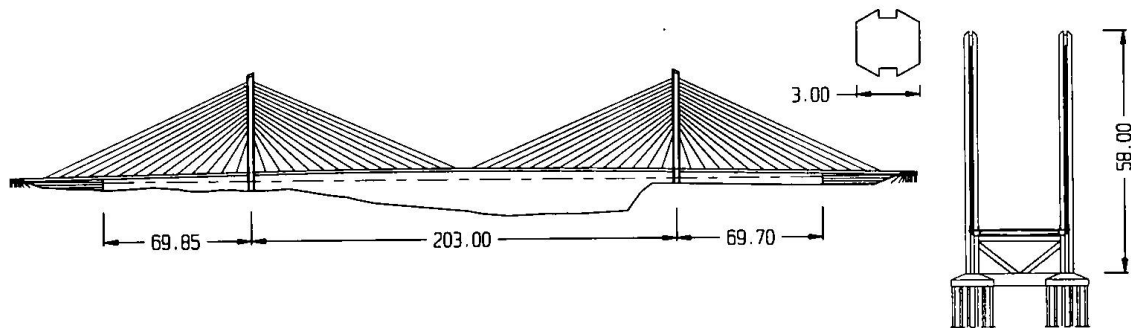


Fig. 1. Papaloapan cable-stayed bridge (bridge and tower elevations; shaft cross section)

The towers are made of two independent shafts which are only linked together by a triangular bracing under the deck. The sense of verticality of these shafts is enhanced by the symmetry of the cable arrangement, the aspect ratio of the shafts (1/19) and their octagonal constant cross-section.

Then, as a result of these conceptual ideas, it was very important to maintain symmetry in all possible aspects of the design and to avoid any interruption in the vertical contour lines of the tower shafts. Cable overlapping in the tower was precluded and there was no room for an interior gallery in the shafts. As a consequence, the natural choice seems to be the use of steel connecting elements between front and back anchorages. The need to maintain vertical contour lines leaves no other choice than embedding these steel elements inside the shafts.

3. Saddle concept

The steel elements which are designed to connect front and back anchorages will be called saddles from now on since their concept is somewhat similar to the saddles of suspension bridges. Their design has to take into account two main constraints: size has to be reduced such as to fit them inside the tower and fatigue resistance has to be excellent since there will not be any possibility for inspection as they are embedded in concrete.

Both reasons made us consider the perforated plate as a suitable concept since it was originally proposed as a good alternative to the stud connector concept for its fatigue strength [6, 7]. Nevertheless important differences may be found between the loads which are applied on a perforated plate shear connector as described previously and our present saddles.

Shear connection is only part of the static problem in the saddles. They also have to transmit tension forces between both stays and vertical compression forces to the concrete tower. A typical design (Fig. 2) consists of a vertical 60 mm thick plate with a double array of 100 mm diameter circular holes, two horizontal 40 mm thick horizontal plates and some additional stiffening plates. Design changes slightly as a function of the slope of the cables. Both anchorages are connected to the vertical plate by means of an intermediate tapered butt-welded cast steel plate whose cross section changes from rectangular to circular in order to be screwed to an annular connector holding the cable anchorage.

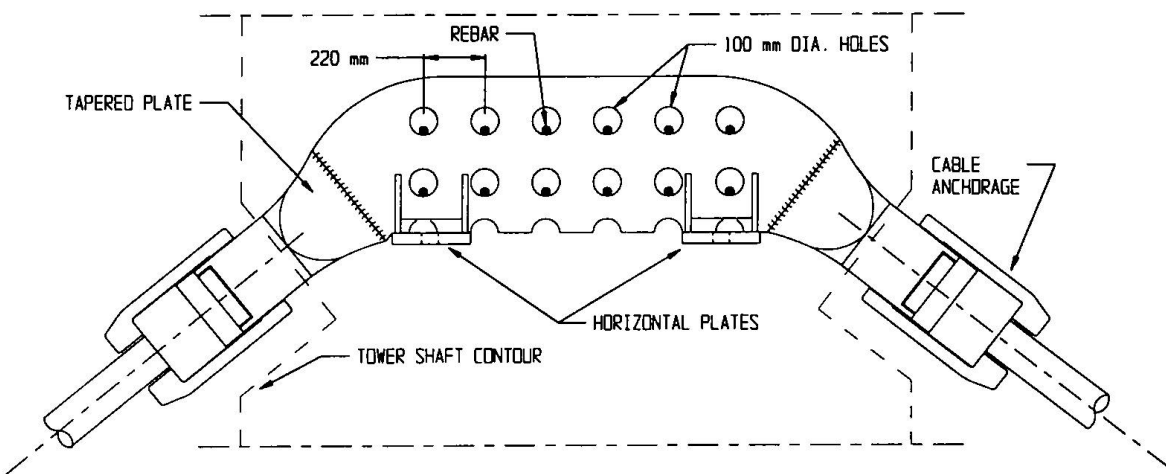


Fig. 2. Saddle elevation.

As compared with perforated plates for shear connection [6,7], these plates are thicker and the holes are also larger. The size of the holes is increased for a number of reasons including the need for large shear strength, the interest in having rebars across the holes and leaving wide enough space for concrete aggregates as well as a better control of stress concentrations in the steel plates. Thickness is much larger than what would be necessary for a shear connector because the vertical plate has to withstand very large tension forces from both stays. All steel elements are made of AH-55 steel (roughly equivalent to AE355) and were stress-relieved by means of a thermic treatment after welding.

4. Saddle design and analysis

4.1 Statical schemes

Among the load cases which have to be considered there are two limit situations which define the resisting properties of the saddles:

- The symmetric load pattern corresponds to roughly similar cable forces on both sides (Fig. 3). In this case the saddles are supporting tension forces and for such load case the stress concentrations around the holes may be very significant. The saddles are also transmitting vertical components to the concrete shaft through the horizontal plates as well as through the shear connectors.
- The unsymmetric load pattern corresponds to unbalanced cable forces; the limit case would be that which happens during erection when only one cable may be stressed (Fig. 3). In this case the saddles are mainly shear connecting devices since they transmit horizontal and vertical forces to the concrete shaft by means of the circular holes as well as through the horizontal plates (in the case of vertical components).

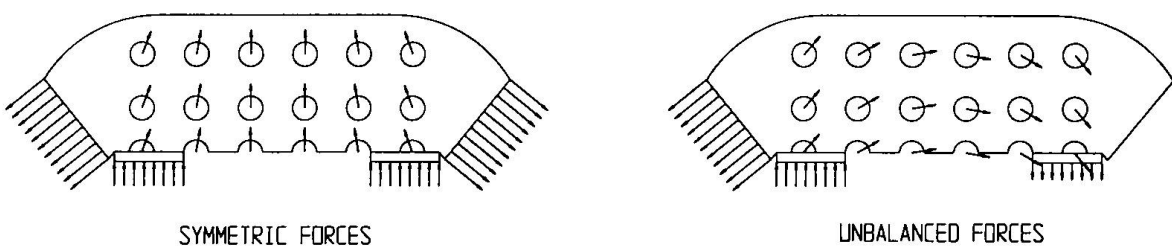


Fig. 3. Basic statical schemes.

Statistical analysis of the saddles could be performed by means of a complete 3D finite element model (Fig. 4). In this model concrete is supposed to be sliding against the steel plate and shear is only transmitted through the concrete dowels. Nevertheless, as complicated concrete cracking patterns make such analysis very unstable, it is difficult to get ultimate strength values. Then such model is only used for elastic analyses. Consequently the static problem has been divided into three parts (the shear connection, the steel plates stresses and concrete stresses) as a way to get a reliable and safe design.

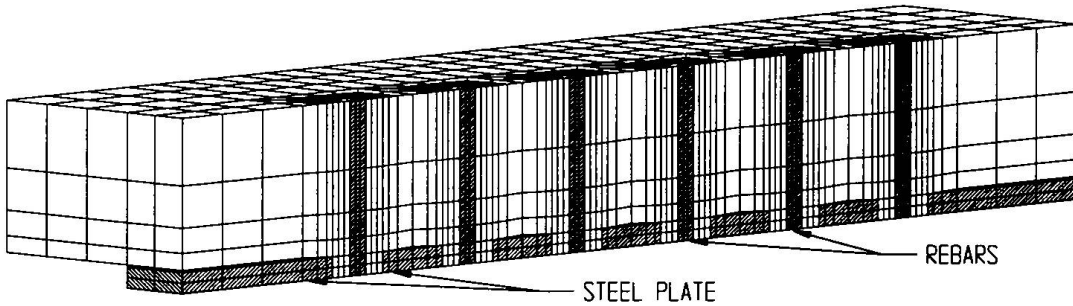


Fig. 4. Three-dimensional finite element model.

4.2 Shear connection

Although previous analytical and experimental studies are available [6, 7], this kind of connection is not yet standard and there are no generally accepted formulas to define its ultimate capacity. If we forget about the plate itself, shear capacity is a function of concrete shear strength (with many limitations because of the complicated geometrical configuration) and of transverse reinforcement as in any standard shear analysis.

This case is somewhat different from the perforated plate with a single array of holes since in that case shear may be transmitted in a fully three-dimensional pattern (normal and parallel to the plate). The multiple array of holes forces shear transmission to concrete only in the normal direction to the plate. The problem is then bi-dimensional and, in some sense, simpler. Several methods have been considered for the design.

If we consider each external plane of the plate as a shear joint and we apply standard design rules such as CEB-FIP [8], Eurocode [9] or ACI [10], the contribution of concrete will be computed as the product of a shear stress and a reference area. Depending on the choice of both factors this contribution could range between 10 and 30 kN for a 100 mm diameter hole and a C40 concrete. The contribution of reinforcement bars is also subjected to different interpretations specially with respect to the coefficient of friction to be applied to the shear transmission plane (it may vary between 0.7 if we consider the contact between the steel plate and concrete and 1.4 for monolithic concrete). A safe estimation of this coefficient of friction (0.9) would give a 608 kN contribution for a 32 mm diameter rebar ($f_{y'd}=420\text{ MPa}$). Then transverse reinforcement is by far the most important factor in defining shear capacity of the connection.

Another limit state which has to be checked corresponds to cracking at inclined angles but this is a more standard computation and it happens to be not as demanding for transverse reinforcement as the previous one. The capacity per hole in the same conditions as before would be 677 kN for the conservative assumption of having cracks at 45°.

Finally the connection has been checked against the dowel action failure. This point might be controversial since reinforcement is embedded in the 100 mm diameter concrete cylinder which is monolithic with the whole shaft. This check gives the most conservative estimation of the connection shear capacity. According to CEB-FIP Model Code [8], the computed capacity would be 217 kN per hole.

Andrä's formulas [7] were also used as an estimation of shear capacity but they have to be taken with care since they have only been shown to be valid for smaller holes and for a three-dimensional shear transmission pattern. Moreover they give the global capacity of the connection including plate failure and our design does not maintain the same scale factor for all geometrical dimensions. As applied here they would predict a 400 kN capacity with a 36 mm rebar per hole which would be converted into 316 kN for our 32 mm diameter rebar.

We finally used the dowel action model as the most conservative estimation. Nevertheless this design process shows how interesting it might be to carry an extensive testing program to define precisely the shear capacity of this kind of connection.

4.3 Steel plate analysis

The second link in the transmission of forces between the cables and the shaft is the plate assembly. To check its state of stress a finite element model has been analyzed (Fig. 5). The most interesting feature of the model may be found in the modelling of the holes. These holes were considered to be filled with concrete and elastically supported at their center. Horizontal plates were also elastically supported at their base. In this way it is possible to obtain a reasonable reaction distribution among the different holes and plates and a reliable stress distribution in the steel plates. Spring constants were evaluated from the three-dimensional finite element analysis which was mentioned earlier (Fig. 4). Resulting value was expressed as $3.1G_c A/D$ (where G_c is the concrete shear modulus, A is the area of the hole and D its diameter) to emphasize the concrete dowel effect which is the origin of this stiffness.

Stress results were checked according to AASHTO Standard [11] in service load design (allowable stress is $0.55 f_y$) and against fatigue (stress variation at any point is limited to a value ranging from 27 to 110 MPa depending on the detail). According to finite element results, maximum stress is by far the governing design criterion; fatigue is not conditioning in any case the design of the saddle (maximum stress variation is only 9 MPa). This result is important since it shows the interest in using this type of connection for a fatigue sensitive structure.

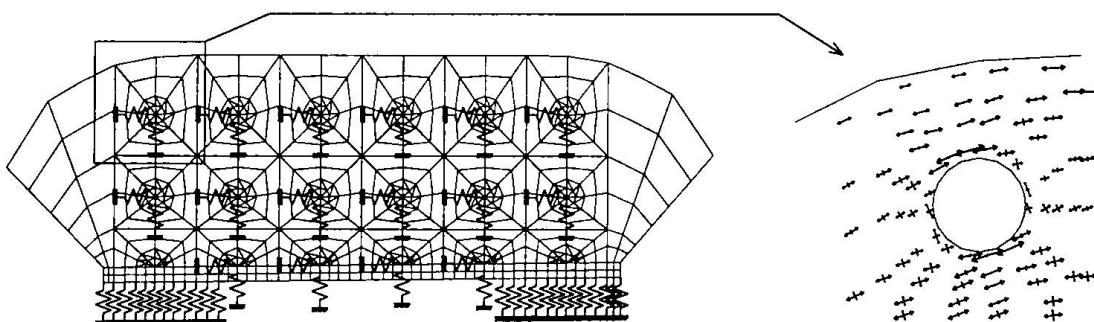


Fig. 5. Finite element model of the plate and detail of stresses.

The stress analysis of the saddles shows the importance of the holes as stress concentrators and the fact that filling with concrete these holes somewhat reduces the stress concentration. If the analysis is repeated after leaving one of the holes empty, maximum von Mises stress is increased by 27%. Then many important reasons support the need for a very careful concrete casting process in order to make the saddle work as it is assumed in the analyses.

With respect to the fatigue strength of this connection it has to be emphasized that the areas of the plate which show a certain fatigue risk are the stress concentrations around the holes. Since the holes are machined and stress relieved afterwards it is very unlikely that residual stresses may be present at these points. Then the fatigue process may be very well controlled through the static analysis of the plate.

4.4 Concrete analysis

Previous analyses lead to reaction forces at all the elastic supports. These reaction forces are input to a new finite element model of the shaft to check concrete stresses. This new analysis does not discover any new aspect of the connection since all the results may be obtained by equilibrium conditions and standard design rules. This analysis shows that tensile stresses develop in the neighbourhood of the saddles due to strain compatibility. Although these stresses are not important, transverse prestressing was arranged in the direction of the saddles to reduce cracking and further increase the fatigue strength of the connection. This transverse prestressing (4 no.36 mm diameter bars per saddle) is in any case much less than what it would be necessary to prestress a hollow shaft to fully transmit cable forces.

5. Conclusions

The perforated plate concept has been selected as a compact and fatigue resistant device to be used simultaneously as a link to transmit tension forces and as a shear connector to absorb unbalanced forces to a concrete structure. Its use in cable stayed bridge towers simplifies design and erection. They are specially interesting for short and medium span bridges where the size of the towers does not leave much space for other connecting devices. A design methodology has been presented but it is too conservative. Extensive experimental testing should be performed to define precisely the strength of such connection.

References

- [1]. Gimsing N.J., "Cable Supported Bridges, Concept and Design", John Wiley & Sons, 1983
- [2]. Schlaich J., "On the Detailing of Cable-Stayed Bridges", Cable-Stayed Bridges, Recent Developments and their Future, ed. M. Ito et al., Elsevier Science Publishers, 1991
- [3]. Haas G., Petersen A. & Ostenfeld K.H., "The Færø Bridges, New Developments in Design and Construction", Int. Symp. on Strait Crossings, Stavanger, 1986
- [4]. Crémer J.M., "Rotation: Original Mode of Erection of the Ben-Ahin Bridge", 13th IABSE Congress Report, pp.975-980, 1988
- [5]. Virlogeux M., "The Normandie Bridge, France: A New Record for Cable-Stayed Bridges", Structural Engineering International 4, pp. 208-213, 1994
- [6]. Leonhardt F., Andrä W., Andrä H.P. & Harre W., Neus, vorteilhaftes Verbundmittel für Stahlverbund-Tragwerke mit hoher Dauerfestigkeit, Beton und Stahlbetonbau, 12, pp. 325-331, 1987
- [7]. Andrä H.P., "Economical Shear Connectors with High Fatigue Strength", IABSE Symposium Brussels, pp. 167-172, 1990
- [8]. CEB-FIP Model Code 1990, Thomas Telford, 1993
- [9]. ENV 1992-1-3, "Design of Concrete Structures", 1991
- [10]. ACI Committee 318, "Building Code Requirements for Reinforced Concrete (ACI 318-89)", 1989
- [11]. AASHTO, "Standard Specifications for Highway Bridges", 1991

Bearing Capacity of Concrete Dowels

Dieter KRAUS

Prof. of Civil Eng.
Universität der Bundeswehr
Munich, Germany

Dieter Kraus, born 1941, obtained his civil engineering degree in 1969 and his Dr.-Ing. degree in 1975 at the Techn. Univ. München. Project engineer in a construction company and Professor for concrete Engineering at the Univ. der Bundeswehr München. Dieter Kraus passed away in March 1997.

Otto WURZER

Civil Eng.
Universität der Bundeswehr
Munich, Germany

Otto Wurzer, born 1964, obtained his civil engineering degree at the Techn. Univ. München. After one year, as a member of construction company, he joined the Univ. der Bundeswehr München as a research Assistant.

Summary

The bearing and deformation behavior of a new shear connector called Concrete Dowel was subject of extensive experimental and theoretical investigations introduced at the University of the German Armed Forces during the last years. The main results of these investigations, a new mechanical model and a draft of a design concept are presented in this paper.

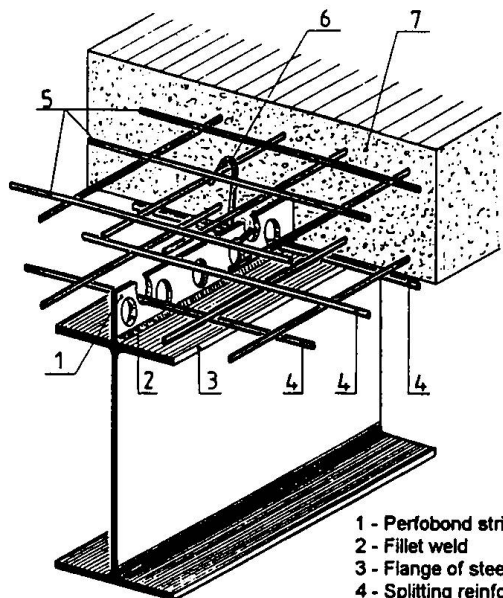
1. Introduction

A new shear connector used for composite beams has been developed since 1986 as „Perfobond Strip“ [1] or „Kombi-Dowels“ [2]. The so called „Concrete Dowels“ are built by parts of the concrete slab interspersing circle or drop shaped holes, which are located in steel strips welded upright on I-sectioned steel girders (Fig. 1). It is also possible to locate these holes directly at the upper edge of the web in L-sectioned steel girders (Fig. 2).

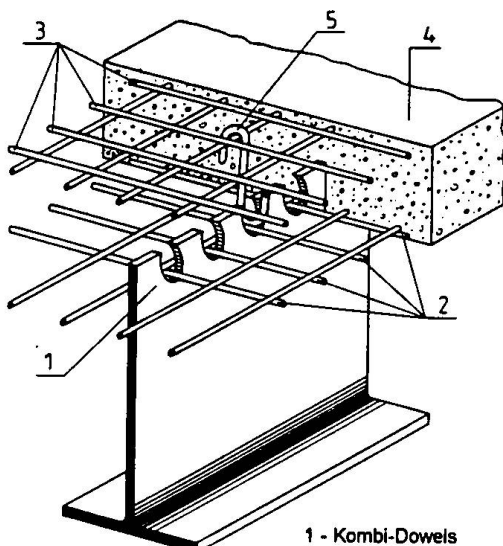
The previous level of knowledge about the bearing behavior of Concrete Dowels is mainly based on tests with small holes [1], [2]. In these tests shear yielding of the steel stems remaining between the holes and local damage of the concrete interspersing the holes were observed as failure criterias. As a simple mechanical model, the concrete interspersing the holes may be considered as to build a dowel loaded to shear and extreme local compression. However the general validity of this model has not been sufficiently proved yet.

As well as the strength, the stiffness and the deformation capacity represent further important properties of a shear connector. The characteristic deformation capacity of small Concrete Dowels (width $b_i \leq 43$ mm) does not justify the assumption of a ductile shear connector, while large Concrete Dowels up to a width of 100 mm showed really ductile load-slip-behavior in initial push-out-tests.

Further extensive experimental and theoretical investigations regarding the bearing and deformation behavior of Concrete Dowels have been introduced at the University of the German Armed Forces during the last years. The states of stress and the failure mechanism causing concrete damage are further important subjects of these investigations as well as the main influence parameters. The main results of these investigations and a draft of a new design concept are presented below. More detailed informations about these investigations are given in [3].



1 - Perforbond strip
 2 - Fillet weld
 3 - Flange of steel girder
 4 - Splitting reinforcement
 5 - Nominal reinforcement
 6 - Vertical tie
 7 - Concrete



1 - Kombi-Dowels
 2 - Splitting reinforcement
 3 - Nominal reinforcement
 4 - Concrete
 5 - Vertical tie

Fig. 1 Composite beam with Perforbond Strip

Fig. 2 Composite beam with Kombi Dowels

2. Experimental Investigations

Altogether 42 push-out-tests using large Concrete Dowels ($h = b; \geq 70 \text{ mm}$) have been executed and evaluated according to Eurocode 4 [4]. Figure 3 shows the typical test specimens and the investigated variant of Concrete Dowels. The influence of the following parameters has been investigated in these tests: material properties of concrete, dimensions and shape of holes and stems, transverse reinforcement, loading of concrete slab.

The typical deformation behavior (load-slip-relation) of Concrete Dowels observed in the tests can be divided in three characteristic sections named I, II, III (see figure 4). At lower load steps (section I) only small deformations occur. According to Eurocode 4 [4] 25 load cycles with an amplitude $\Delta P \approx 0,35 P_{\max}$ have been introduced in this section to remove the adhesion between steel strip and concrete slab. Longitudinal splitting cracks occur in the concrete slab at a load level $P_{\text{crack}} \approx 0,75 P_{\max}$, which cause a sharp increase in deformation with further rising load (section II).

The maximum shear resistance P_{\max} is reached, when local parts of the slab surface are wedging off close to the Concrete Dowels. After reaching P_{\max} shear resistance is decreasing slowly with further deformation and progressive concrete erosion (section III).

At the end of the tests some of the concrete slabs have been longitudinally cutted to examine the condition of the concrete dowels (see figure 5). The concrete interspersing the holes seemed to be locally damaged. Wedges of completely compacted concrete, which have been found close to the contact surface, must be particularly mentioned.

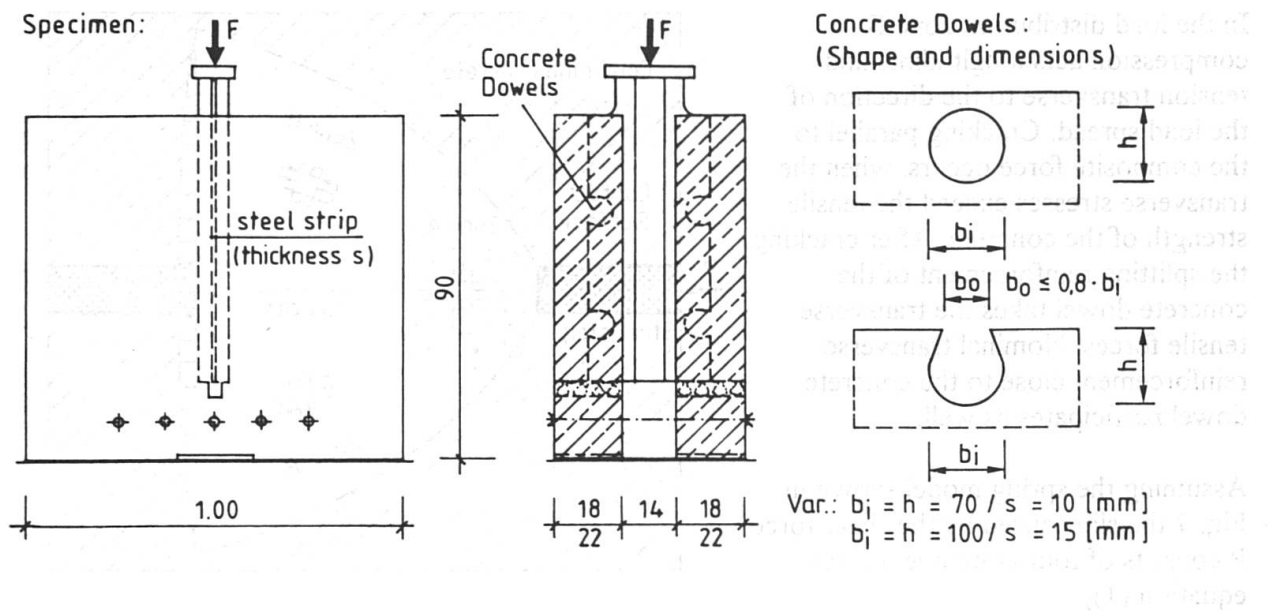


Fig. 3 Push-out test specimen and investigated variants of Concrete Dowels

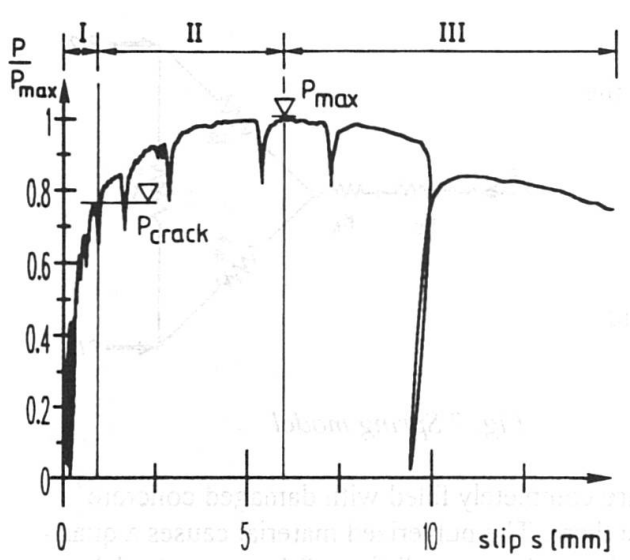


Fig. 4 Characteristic deformation behavior

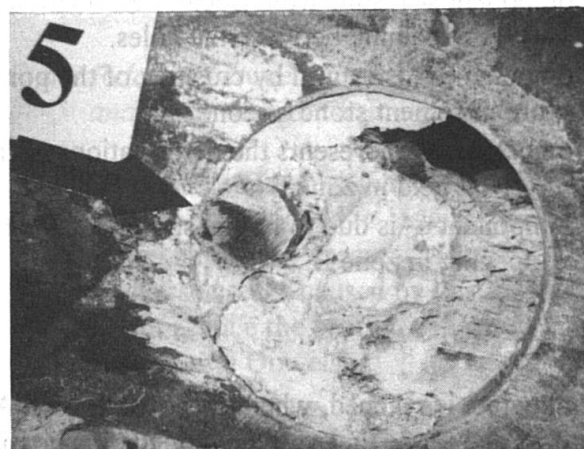


Fig. 5 State of damage

3. Mechanical Model

The composite force is transmitted from the steel strip to the concrete slab by extreme local compression (effect of partial area loading), which acts at the contact surfaces of the hole. The area, where the load spread is taking place in the concrete dowel, may be separated in two main parts named zone A and zone B (see Fig. 6).

In the load transmission zone A concrete is confined causing triaxial compression. There the bearing and deformation behavior of the concrete depends mainly on the pore structure of the cement stone. Above a critical load step crushing of pore sides occurs caused by the triaxial compression. Afterwards damaged concrete material fills up the pores.

In the load distribution zone B compression acts longitudinal and tension transverse to the direction of the load spread. Cracking parallel to the composite force occurs, when the transverse stresses exceed the tensile strength of the concrete. After cracking the splitting reinforcement of the concrete dowel takes the transverse tensile forces. Nominal transverse reinforcement close to the concrete dowel participates as well.

Assuming the spring model shown in Fig. 7 the slip caused by the shear force P consists of four components (see equation (1))

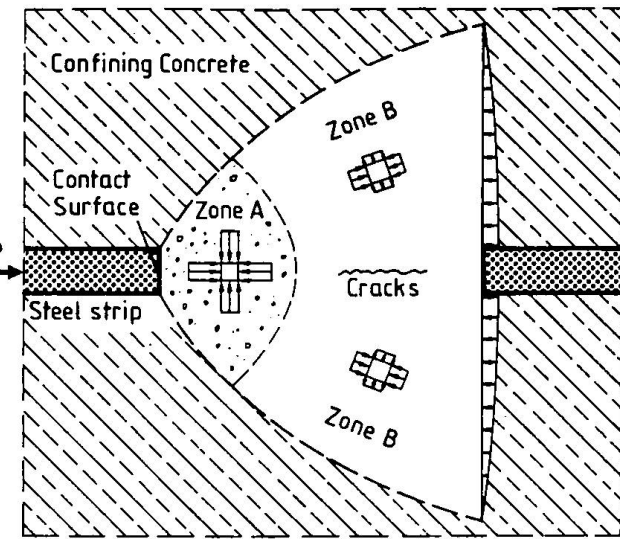


Fig. 6 Loading of a Concrete Dowel

$$s_{(P)} = s_s + s_A + s_B + s_c \quad (1)$$

- Component s_s results from (local) deformation of the steel stems remaining between the holes.
- Component s_A is caused by crushing of the pore structure in cement stone of zone A
- Component s_B represents the deformations of the compression field in zone B
- Component s_c is due to lateral strain, cracking and crack opening in zone B

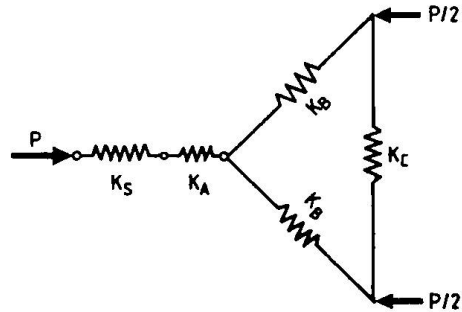


Fig. 7 Spring model

A limit state is reached, when the pores in zone A are completely filled with damaged concrete material and no further volume reduction is possible there. The pulverized material causes a quasi-hydrostatic pressure on the confining concrete, which may lead to splitting of the concrete slab and finally to local wedging off of parts of the slab surface close to the dowels.

The validity of the presented mechanical model has been successfully proved using nonlinear finite element analyses. The main conditions and results of these FE-analyses are given in [5].

4. Significant parameters

The tests resulted a nearly linear relation between the compressive strength f_{cm} and the shear resistance P_{max} of Concrete Dowels (see figure 8). Figure 8 shows as well the effect of an increase in transverse reinforcement A_{eq} , which rises the shear resistance P_{max} of Concrete Dowels. Reinforcing bars positioned inside the holes take most effect there.

The shear resistance P_{max} of Concrete Dowels rises with increasing dimensions. Assuming the mechanical model described in chapter 3, the shear resistance P_{max} depends considerably on the area A_L of the contact surface, where load transmission acts between steel strip and concrete slab.

Therefore the depth h of the holes and the thickness s of the steel strip must be considered as the essential dimension parameters. However, in the presented tests a decrease of the ultimate local compressive stresses f_{cc} transmitted in the contact surface has been observed with increasing A_L . As shown in figure 9 as well, the ultimate values f_{cc} of large Concrete Dowels have not been considerably influenced by the shape of the holes.

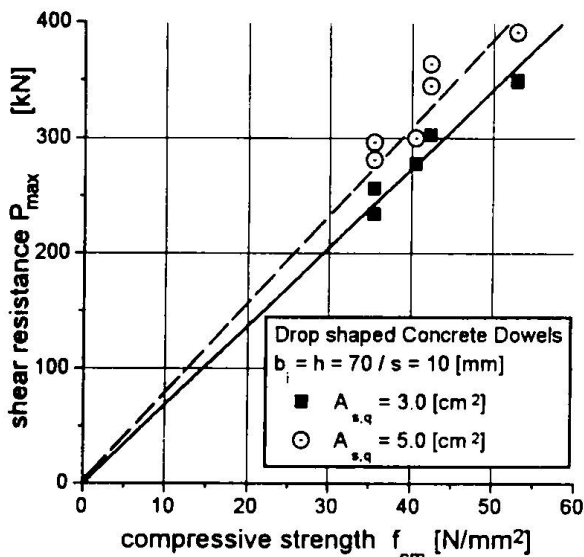


Fig. 8 Relation between concrete strength and shear resistance

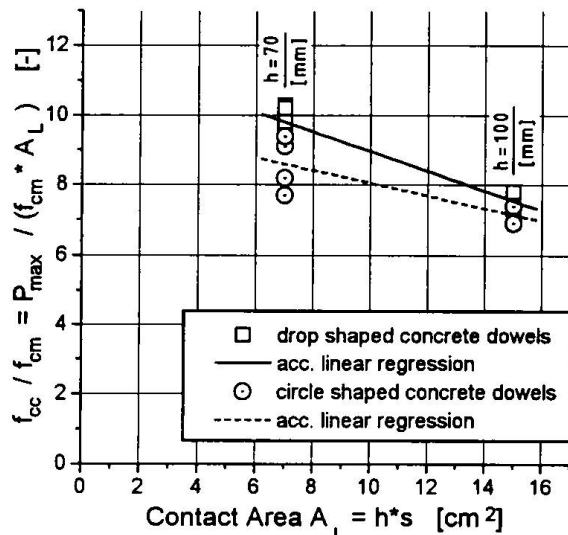


Fig. 9 Relation between dimensions and shear resistance

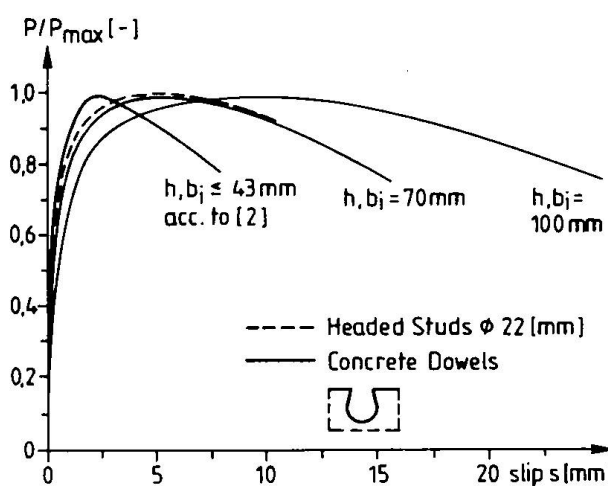


Fig. 10 Characteristic load-slip-relations

In the presented investigations the pore volume of the cement stone was recognized as an important parameter for the deformation behavior of Concrete Dowels, but no influence of the compressive strength f_{cm} of concrete was observed in these tests.

The deformation behavior of Concrete Dowels was getting more ductile with increasing dimensions (see figure 10). Concrete Dowels with dimensions $h = b_i = 70$ [mm] showed a similar deformation behavior like stud shear connectors with a diameter $\phi = 22$ mm. But only a small influence of the shape of the holes was found especially for large Concrete Dowels.

In addition some push-out-tests with concrete slabs loaded to longitudinal tension have been executed. But the transverse cracks caused by this loading did not reduce the bearing capacity P_{max} of the Concrete Dowels.

The loading of the concrete slab by a (negative) transverse bending moment rises the bearing capacity of Concrete Dowels similar to the conditions of stud shear connectors. A transverse bending moment $m_q = -19,0$ [kNm/m] loaded to the concrete slabs of some specimens caused a 35% increase in bearing capacity P_{max} of Concrete Dowels.

The results of the push-out tests were evaluated according to Eurocode 4 [4]. The characteristic deformation capacity δ_{uk} amounts about 8,0 [mm] for the Concrete Dowels with $h = b_i = 70$ [mm] and $\delta_{uk} \geq 10$ mm for the one with $h = b_i = 100$ [mm]. Therefore a Concrete Dowel with dimensions $h = b_i \geq 70$ [mm] may be considered as a ductile shear connector, because it fulfills the criterion $\delta_{uk} \geq 6,0$ [mm] according to [4].

All other parameters (transverse reinforcement, loading of concrete slab) showed only small influence on the deformation behavior of the Concrete Dowels.

5. Design Concept

Based on the mechanical model presented in chapter 3 the design shear resistance P_{Rd} of Concrete Dowels in the ultimate limit state (acc. to [4]) can be determined from equation (2). The factor η in equation (2) depends on the dimensions and the shape of the Concrete Dowels and also on the transverse reinforcement. For example $\eta = 6,8$ was evaluated for drop shaped Concrete Dowels with $h = b_i = 70$ [mm], $b_o/b_i = 0,8$, $s = 10$ [mm], which requires a transverse reinforcement determined for the tensile force $F_s = 0,5 P_{Rd}$.

$$P_{Rd} = \eta \cdot f_{ck} \cdot h \cdot s \cdot \frac{1}{\gamma_v} \quad (2)$$

where:

- f_{ck} the characteristic cylinder strength of the concrete
- h height of the holes of Concrete Dowels
- s thickness of the steel strip
- γ_v partial safety factor; $\gamma_v = 1,25$ according to [4]
- η factor, found by statistical evaluation of test results

References

- [1] Andrä, H.P.: Economical Shear Connectors with High Fatigue Strength. IABSE Symposium „Mixed Structures including New Materials“. IABSE-Reports Vol. 60, pp. 167-172, Brussel 1990.
- [2] Bode, H.: Gutachterliche Stellungnahme zum Antrag auf bauaufsichtliche Zulassung der Kombi-Verdübelung (expert-report on the application for general approval of small Kombi-Dowels). Not published.
- [3] Wurzer, O.: Bearing Capacity of Concrete Dowels. Research report. Universität der Bundeswehr München; in preparation.
- [4] Eurocode 4: Design of composite steel and concrete structures.
- [5] Kraus, D., Wurzer, O.: Nonlinear Finite Element Analysis of Concrete Dowels. Computers & Structures. Vol. June 1997.

Fatigue in Stud Shear Connectors

N. GATTESCO

Assistant Professor

Department of Civil Engineering
University of Udine, Italy

Natalino Gattesco, born in 1958, obtained his engineering degree in 1983 at the University of Udine. He is assistant professor at the University of Udine. His main research interests concern composite beams under cyclic loads, nonlinear analysis of concrete structures, bolted connections in wood elements and structural strengthening of existing masonry structures.

Summary

The results of a numerical simulation of the behavior of steel and concrete composite beams subjected to cyclic loads are here presented. Both partial and complete shear connections were considered. The results show that no significant differences in slip occur with partial interaction. Two groups of beam specimens were numerically tested concerning either connectors distributed according to the longitudinal shear loads or uniformly spaced. The second group showed values of the slip considerably greater.

1. Introduction

In steel and concrete composite beams subjected to cyclic loads a particular attention has to be paid to the connection because it may reach a premature failure due to fatigue. If the connection during loading cycles remains in the elastic range a large number of cycles is needed before it collapses (high-cycle fatigue) on the contrary, if inelastic deformations of the connection are involved, the failure may occur after a limited number of cycles (low-cycle fatigue).

Normally the connections are designed to be able to transmit a longitudinal shear force equal to the difference between the resisting longitudinal forces, in either the steel member or the concrete slab (the lesser), at two adjacent sections of maximum moment or free end (complete shear connection). However, sometimes it is useful or necessary to provide a partial shear connection. In fact, when precast elements are used for the concrete slab it is quite difficult to obtain complete shear connections because for constructional needs only limited space is available to allocate the connectors. Moreover, often the composite system is needed mainly to increase the stiffness of the structure so that a complete shear connection may cause an excessive resistance.

Current codes [1] for composite bridges do not allow the use of partial shear connections and moreover the connectors have to be spaced according to the longitudinal shear force so as to enable the use of the constant stress approach for fatigue. This approach is based on the hypothesis of linear elastic behavior of elements (high-cycle fatigue approach).

As a matter of fact, the load-slip relationship of the connector is nonlinear even for very low values of the load. Moreover at the end of the reloading branch of each cycle an increment of slip Δs_0 is accumulated due to the progressive damage both in the concrete in front of the stud and in the shank of the stud.

On the basis of such considerations the scope of the present research is to simulate the connector behavior in a beam by means of a numerical procedure. The investigation concerns bridge-type beams subjected, for simplicity, to a cyclic uniformly distributed load and arranged with different

degree of connection in order to check if partial shear connection is really unproposeable for bridges.

To emphasize the problem a low-frequency heavy load was considered as reference in the simulations so to involve significant nonlinear displacements.

Moreover such a procedure allows to obtain the slip history of the studs in the beam which is indispensable for the experimental study of the resistance of studs to fatigue when significant inelastic deformations are involved. In fact, as stated in [2], in these cases the tests have to be performed using a strain-control procedure instead of the common stress-control one. The slip history used in that paper [2] was obtained with the same numerical procedure but using a more rough load-slip relationship for connectors [3].

2. Numerical model.

A numerical approach based on the four noded finite element of Fig. 1 was adopted in the simulation [3]. Each element has 12 degrees of freedom which become 8 if the uplift of concrete slab is neglected and the curvature of concrete element and steel beam are the same.

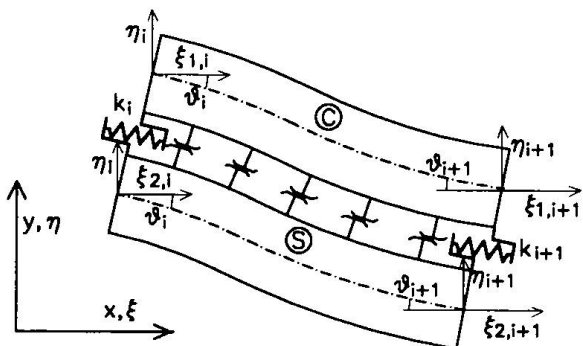


Fig. 1 - Four noded finite element.

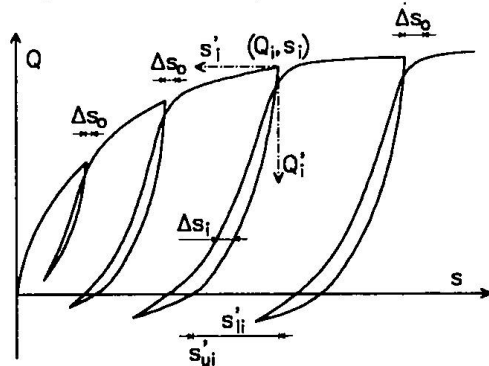


Fig. 2 - Load-slip curves (Q - s) of a connector for repeated loading.

The concrete (C) and the steel (S) are assumed as linear elastic materials while for the connection the following load-slip relationships are assumed [3,4]. In particular the monotonic curve is described by the function

$$Q = \alpha \cdot (1 - e^{-\alpha}) + \gamma \cdot s \quad (1)$$

where Q is the shear force of the connector, s is the slip between the concrete slab and the steel beam and the coefficients α , β , γ are constants to be experimentally determined.

The unloading curves refer to a local axis with the origin in points (Q_i, s_i) where the unloading starts (Fig. 2).

$$Q'_i = Q_i \cdot \lambda \cdot (1 - e^{-\frac{\eta \cdot z_i}{\lambda}} + \frac{\delta}{\lambda} \cdot z_i) \quad (\text{with } z_i = \frac{s'_{li}}{s'_{ui}}) \quad (2)$$

where s'_{li} is the slip, referred to the local axis, corresponding to a zero value of the load and it depends to the shear load Q_i

$$s'_{li} = c_1 \cdot Q_i^3 + c_2 \cdot Q_i, \quad (3)$$

η has the following expression

$$\eta = b_1 \cdot Q_i - b_2. \quad (4)$$

The coefficients λ (Eq. 2), c_1 , c_2 (Eq. 3) and b_1 , b_2 (Eq. 4) have to be experimentally determined. The value of coefficient δ is obtained by Eq. 2 imposing $Q'_i = Q_i$ for $z_i = 1$ ($s'_i = s'_{li}$). The value of the slip at the end of the unloading s'_{li} varies with the number of cycles according to the relationship [4]

$$s'_{li}^j = s'_{li}^1 \cdot (1 + \rho \cdot \frac{(j-1)^\varepsilon}{25 + (j-1)^\varepsilon}) \quad (5)$$

where ρ and ε are constants and the suffix j means cycle number j .

The reloading curves are referred to the same local axis. Each point of the curves is obtained by an horizontal translation Δs_i (Fig. 2), starting from the unloading curve, which depends on s'_{ui} according to the relationship

$$\Delta s_i = \xi \cdot (s'_{ui} - s'_{li}), \quad (6)$$

where s'_{ui} represents the slip value at the beginning of the reloading. ξ can be expressed as a function of s'_{li}/s'_{ui} in the following way

$$\xi = c_3 \cdot (1 - e^{-\frac{c_4 \cdot z_i}{c_3}}) + c_5 \cdot z_i + c_6, \quad (7)$$

c_3 , c_4 , c_5 are constants and c_6 has the relationship

$$c_6 = \frac{\Delta s_{oi}}{s'_{ui}}. \quad (8)$$

The increment in slip Δs_{oi} at the end of the reloading curve, which represents the cumulative damage at each cycle, may be determined in this way

$$\Delta s_{oi}^j = \frac{Q_i \cdot s'_{ui}^j}{s'_{li}^j} \cdot \left(\frac{\nu - \mu}{j} + \mu \right) \quad (9)$$

where ν and μ are constants. The coefficients c_3 and c_4 vary with the number of cycles in the following way

$$c_3^j = c_3^1 - \left(\frac{\Delta s_{oi}^1}{s'_{ui}^1} - \frac{\Delta s_{oi}^j}{s'_{ui}^j} \right) \quad (10)$$

$$c_4^j = \frac{c_3^j}{c_3^1} \cdot c_4^1. \quad (11)$$

3. Specimen details.

The study concerns simply supported bridge-type beams with the geometric characteristics illustrated in Fig. 3. The yielding stress of structural steel was $f_{ys} = 355$ MPa ($\gamma_s = 1.00$), and the

compressive strength of concrete was $f_{ck} = 30 \text{ MPa}$ ($\gamma_c = 1.50$). The coefficients needed to describe the load-slip of connectors under repeated loads were derived from experimental results [5] and they are reported in Table 1. Also the geometric and mechanical characteristics of stud connectors are indicated in the same table.

Characteristics of studs		Load-slip relationship coefficients			
Shank diameter	$\phi = 19 \text{ mm}$	Monotonic curve	Unloading curves	Reloading curves	Damage parameters
Yielding stress	$f_y = 350 \text{ MPa}$				
Ult. tensile strength	$f_t = 450 \text{ MPa}$	$\alpha = 82 \text{ kN}$ $\beta = 230 \text{ kN/mm}$	$\lambda = 0.90$ $b_1 = 0.054 \text{ kN}^{-1}$ $b_2 = 1.34$	$c_3 = -c_6$ $c_4 = 2.3$ $c_5 = 0.4$	$\varepsilon = 0.85$ $\rho = 0.31$ $v = 1.16 \cdot 10^{-4} \text{ mm/kN}$ $\mu = 1.7 \cdot 10^{-5} \text{ mm/kN}$
Concrete comp. strength	$f_{ck} = 30 \text{ MPa}$	$\gamma = 5 \text{ kN/mm}$	$c_1 = 9.2 \cdot 10^{-7} \text{ mm/kN}^3$	$c_2 = 9.0 \cdot 10^{-4} \text{ mm/kN}$	
Exp. stud capacity [4]	$Q_u = 100 \text{ kN}$				

Table 1 - Characteristics of stud connectors and load-slip relationship coefficients.

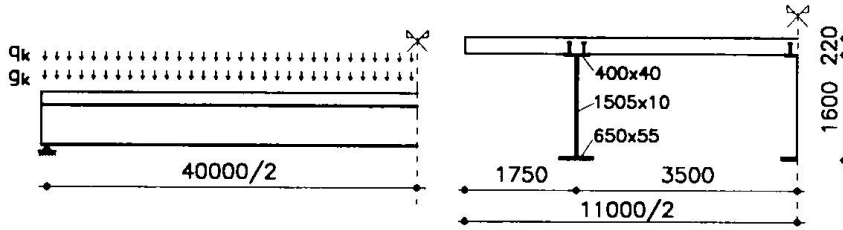


Fig. 3 - Geometrical characteristics of bridge-type beam considered.

As aforesaid the beam was subjected to cyclic uniformly distributed loads which vary between zero and a maximum value. It is supposed that the structure be built without the use of props so that the own weight g_k of the composite beam was supported by the steel member alone. The own weight ($g_k \sim 25 \text{ kN/m}$ per each single beam), then, was not considered in the analyses.

Five different degrees of shear connection were assumed for the beams ($N/N_f = 0.6 \div 1.0$) and the connectors were arranged either following the longitudinal shear diagram (triangular distribution) or equally spaced (uniform distribution).

The load applied to the beams with complete shear connection was the maximum service load (on a single beam) for a three lane bridge according to the Italian code ($q_k \sim 56 \text{ kN/m}$). The steel member, the concrete slab and the connection were designed on the basis of the ultimate load associated to the cited service loads ($\gamma_G = 1.35$, $\gamma_Q = 1.50$).

The same geometric characteristics for concrete slab and steel beam were assumed for the specimens (beams) with partial shear connection. The load applied was derived from the equilibrium method [1] on the critical section (maximum moment). The loads evaluated in this way are reported in Table 2.

4. Results

The numerical simulations concern bridge-type beams with five different degrees of connection and with two types of arrangement of studs along the span (triangular and uniformly distributed). The analyses were conducted up to 2000 cycles so as to investigate if the solutions tend to an almost stable value, in terms of slip or shear force, in the connection. It has to be noted that the Eq. (9), representing the cumulative damage in the connection, do not include the fast increase in damage which precede the stud failure [5,6]. So that the results which can be obtained with such a

N/N_f	Number of studs	Load q_k [kN/m]	s_{\max}^1 [mm]	s_{\min}^1 [mm]	s_{\max}^n [mm]	s_{\min}^n [mm]	s_{\min}^n / s_{\max}^n
Beams with studs arranged as the longitudinal shear							
1.00	255	56.00	0.311	0.161	0.612	0.420	0.685
0.90	230	54.12	0.356	0.179	0.643	0.406	0.631
0.80	204	52.16	0.417	0.220	0.690	0.398	0.577
0.70	179	49.07	0.483	0.264	0.736	0.384	0.520
0.60	153	44.56	0.545	0.307	0.771	0.363	0.470
Beams with studs equally spaced							
1.00	255	56.00	0.990	0.345	1.266	0.462	0.365
0.90	230	54.12	1.160	0.397	1.420	0.482	0.340
0.80	204	52.16	1.407	0.477	1.650	0.515	0.312
0.70	179	49.07	1.658	0.562	1.880	0.559	0.297
0.60	153	44.56	1.860	0.627	2.057	0.585	0.285

n is equal to 2000 cycles.

Table 2 - Results concerning the beams studied.

simulation are reliable up to 2/3÷3/4 of the connector life.

The results concerning the distribution of studs according to the longitudinal shear force (triangular distribution) are plotted in Fig. 4a. In particular in the figure the variation of the maximum slip of the extreme connectors with the number of cycles is shown. It is possible to note that the slip increases significantly in the first 300÷400 cycles and then tends to an almost constant value. The minimum slip (value of the slip at each load removal) varies similarly to the maximum slip as can be seen in Table 2.

The increase in maximum slip is less pronounced for partial shear connections ($N/N_f = 0.6$ - $s_{\max}^n / s_{\max}^1 = 1.41$) than for complete shear connection ($s_{\max}^n / s_{\max}^1 = 1.97$). So that the difference between the maximum slip at $n = 2000$ cycles of the beam with degree of connection $N/N_f = 0.6$ and that of the beam with full interaction ($N/N_f = 1.0$) is quite limited (~1.26).

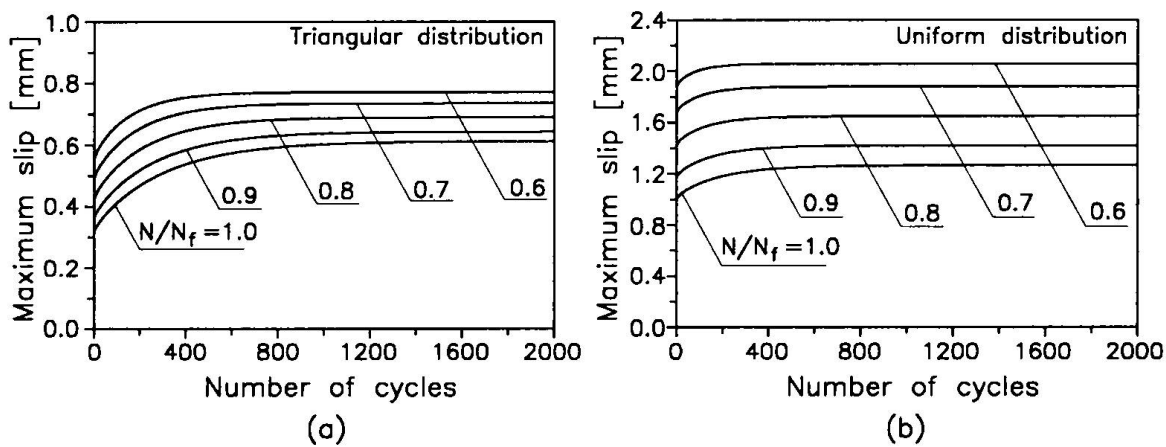


Fig. 4 - Maximum slip versus number of cycles: triangular a) and equally spaced studs b).

This results seems to indicate that the partial shear connection is not a solution very much worse than the full interaction one.

The increase in maximum slip is less pronounced for partial shear connections ($N/N_f = 0.6$ - $s_{\max}^n / s_{\max}^1 = 1.41$) than for complete shear connection ($s_{\max}^n / s_{\max}^1 = 1.97$). So that the difference

between the maximum slip at $n = 2000$ cycles of the beam with degree of connection $N/N_f = 0.6$ and that of the beam with full interaction ($N/N_f = 1.0$) is quite limited (~ 1.26).

This results seems to indicate that the partial shear connection is not a solution very much worse than the full interaction one.

In Table 2 are also reported the peak values of the slip (s_{\max} , s_{\min}) of the extreme connectors of the beam both at the first cycle and at the 2000-th cycle. In the last column of the table the values of the ratio between the minimum and the maximum slip at the 2000-th cycle are reported.

The curves of the maximum slip versus the number of cycles for beams with equally spaced connectors are plotted in Fig. 4b. Also these curves tend to an almost constant value of the slip after 2000 cycles. The increase in slip with cycles is more limited than in Fig. 4a because a greater redistribution of the shear force along the span is possible (the connectors close to midspan are initially very little engaged).

The principal results are summarized in Table 2. The values of the slip in these cases are significant and then considerable inelastic deformations are involved in the connectors at each cycle so that it is likely to occur the failure of the connectors after a low number of cycles (low-cycle fatigue) [2].

The loads considered are heavy repeated loads which may be present on the bridge only some thousands times during the structure life but the scope of the research was to investigate the effects under such severe loads. Actually at these loads all the other loads with higher frequency has to be added and then to consider the combined effect.

5. Conclusions

The study refers to low-frequency heavy loads and considers five different degrees of connection. The results evidence that there is a considerable increase in slip in the first 300-400 cycles and then it tends to an almost constant value.

The changes between different degrees of interaction, in case of triangular distribution of the studs, are not very large so that it seems reasonable to consider partial shear connections also for bridges.

The case with equally spaced connectors indicate very large values of the slip even in the case of complete shear connection.

This early results are part of a study which aims to increase the knowledge on the problem of fatigue in the connection of composite systems. Moreover this results provide important information on the slip history of the connectors in the beam which is needed to perform strain-control experimental tests on single connectors [2].

Acknowledgement. Thanks to prof. Ezio Giuriani for the time spent in stimulating discussion.

References

- 1 Eurocode No. 4: Design of Composite Steel and Concrete Structures. Part 1.1: General Rules and rules for Buildings. (March 1992) and Part 2: Bridges. (July 1996).
- 2 Gattesco N., Giuriani E., Gubana A., "Low-Cycle Fatigue Test on Stud Shear Connectors", Journal of Structural Division, ASCE, 123 (2), 1997.
- 3 Gattesco N., Giuriani E., "Analysis of steel and concrete composite beams under repeated loads", Technical Report of the University of Udine (Italy), IMTA No.7, Dec.1990.
- 4 Gattesco N., "Load-Slip Relationship of the Connectors Under Repeated Loads", in preparation.
- 5 Gattesco N., Giuriani E., "Experimental study on stud shear connectors subjected to cyclic loading", Journal of Constructional Steel Research, 38 (1), pp. 1-21, 1996.
- 6 Mainstone R.J., Menzies J.B., "Shear connectors in steel-concrete composite beams for bridges: Part 2, Fatigue tests on beams", Concrete, Vol. 1, No. 10, Oct. 1967, pp.351-358.

Incremental Slip of Stud Shear Connectors under Repeated Loading

Geoff TAPLIN

Senior Lecturer
Monash University
Melbourne, Australia

Geoff Taplin has research interests in the slip behaviour of composite slabs, incremental collapse of composite beams under repeated loading, early history of reinforced concrete, and engineering education.

Paul GRUNDY

Professor of Struct. Eng.
Monash University
Melbourne, Australia

Paul Grundy is Professor of Structural Engineering and Head of the Department of Civil Engineering at Monash University. He has research interests in the shakedown behaviour of structures, tubular connections, and ship hull integrity.

Summary

A test to measure the incremental slip of stud shear connectors under repeated loading is described. Results of both symmetric and unidirectional cyclic load tests are presented, together with empirical equations for the rate of slip growth as a function of load.

1. Introduction

Incremental slip between the concrete slab and the steel beam in a composite beam constructed with stud shear connectors has been observed by a number of researchers while undertaking fatigue testing of shear studs, but relatively few have focussed on the importance of incremental slip in its own right, and attempted to quantify the slip behaviour as a function of load and number of cycles (see for example Hallam (1976), Hawkins & Mitchell (1984), Oehlers & Carroll (1987), Oehlers & Coughlan (1986)). Incremental slip occurs due to crushing of the compression concrete ahead of the shear stud, and yielding of the shear stud.

Under monotonic loading this slip is not detrimental to the behaviour of a composite beam, but rather it is beneficial because it provides the ductility in the shear connection which allows loads to be redistributed at the ultimate limit state. Under repeated loading, however, the slip accumulates with each cycle of load. If the slip increments reduce with load cycles, the slip will stabilise, and the beam can be considered to have "shaken down" to a stable equilibrium condition. If the slip increments are constant or increase with each cycle of load, then shakedown will not occur, and incremental collapse of the beam will result. A serviceability failure of the structure is the likely outcome of this latter situation.

An experimental investigation of the shakedown behaviour of composite beams conducted at Monash University (Thirugnanasundaralingam 1991) showed that incremental collapse occurred at loads as low as 53% of the static collapse load. It is clear, therefore, that guidance is needed for designers on the shakedown loads for composite beams, and the rate at which incremental slip (and hence incremental beam deflection) will occur if the shakedown load is exceeded. To meet this need, a series of tests have been undertaken on composite beam specimens with the specific aim of quantifying the incremental slip behaviour, and obtaining an empirical relationship between the level of cyclic load and the rate of slip growth per load cycle.

2. Test set up

Many authors have discussed the requirements for a test set up that will give a true representation of the strength of shear studs in composite beams (see for example Viest (1956), Chapman (1964), Mainstone & Menzies (1967), Davies (1967a and b), Goble (1968), Ollgaard, Slutter & Driscoll (1971), Hawkins (1973), Johnson & Oehlers (1981), Maeda, Matsui & Hiragi (1983) and Gattesco & Giuriani (1996)). From this work, the “push-out” test has evolved as the standard test for the strength of stud shear connectors. The parameters of the test are described in various codes of practice (see for example Eurocode 4 (ENV 1994-1-1: 1992)). The test has gained acceptance despite the long recognised fact that prying forces are developed across the concrete-steel interface, resulting in tension in the shear studs. Therefore, the test can be considered as a standardised measure of shear stud performance, rather than an accurate reproduction of the behaviour that occurs in a composite beam. An analogy would be the cube or cylinder test for concrete, which has developed as a standard test despite the fact that the loading conditions for concrete in a beam situation are not accurately reproduced in the standard test.

In undertaking this investigation into the incremental slip of shear stud connectors under repeated load, an early decision had to be made as to whether to undertake the investigation using a test rig that would reproduce as accurately as possible the conditions in a composite beam, or to use the “push-out” test, adapted for cyclic loading, and accept the known differences between the test conditions and the situation that exists in a composite beam. The push-out test was adopted for this testing programme, because it was considered that, just as it has gained acceptance with industry as a standardised measure for the static strength of a shear stud, it has the potential to be accepted as the standard test for the incremental slip behaviour under repeated loading.

2.1 The test specimens

The two concrete slabs used for each push-out test were 450 mm (in the direction of the applied load) by 500 mm x 90 mm thick. Each slab was connected to the flange of a steel I beam with four 12.5 mm diameter by 50 mm headed shear studs. The studs were arranged in two rows with a lateral spacing of 65 mm (5.2 diameters). The longitudinal spacing was 50 mm. To prevent longitudinal splitting, the slabs were reinforced with two layers of 8 mm wires at 100 mm centres. Maeda, Matsui & Hiragi (1983) have identified the need for each pair of slabs to be cast horizontally with the shear studs vertical. Various researchers have used different methods to achieve this, including casting the slab for one side of the push-out specimen, inverting the specimen when the concrete has hardened sufficiently, and casting the other slab. This has the disadvantage that each specimen is by necessity cast from a separate concrete mix, and given the variation that occurs in concrete strength between mixes, the two slabs will very likely have slightly different properties. Another method that has been adopted is to cast the slabs onto separate steel plates which, when welded to a third plate, form the flanges and web of an I beam. In this research program, a modification of this procedure was undertaken whereby the studs were welded to a 20 mm plate. Each plate was subsequently connected to a flange of a rolled steel I beam by bolting the plate to the beam flange with 10 high strength 12 mm bolts. This procedure met the objectives of casting the specimens horizontally with the studs vertical, and from the same concrete mix, but avoided the need for expensive and time consuming welding as part of the specimen preparation. The plate was greased prior to casting to remove friction between the concrete and the steel.

2.2 The test rig

A purpose built reaction frame was constructed for these tests (Figure 1). Because the



Figure 1: Test rig and specimens

specimens were tested under cyclic load, the specimens were clamped between steel plates and the reaction frame acted in both tension and compression. The steel plates provided horizontal restraint to the slabs on their compression edge by friction between the concrete and the steel. The specimens were loaded by a 100 kN servo controlled Instron hydraulic actuator. Monotonic tests were conducted under displacement control (0.6 mm per minute) and the cyclic load tests were tested under load control, so that incremental slip measurements could be obtained. Slip between each slab and the steel plate to which it was connected was measured directly via a linearly variable differential transformer mounted on the steel plate and reacting against a bracket on the concrete slab. The compliance of the load frame, and any potential slip in the bolted connection between the steel plate and the steel I beam was therefore excluded from the slip measurements.

3. Test results

3.1 Monotonic tests

Four specimens were tested under monotonic loading to establish the static strength of the stud shear connectors, P_u . The results of those tests are presented in Table 1 below.

Test number	Ultimate load per stud, P_u (kN)	Slip at ultimate load (mm)
2	47.4	
7	50.8	6.11
8	46.0	5.11
10	52.4	6.11
average	49.2	5.78

Table 1: Monotonic test results

3.2 Symmetric cyclic test results

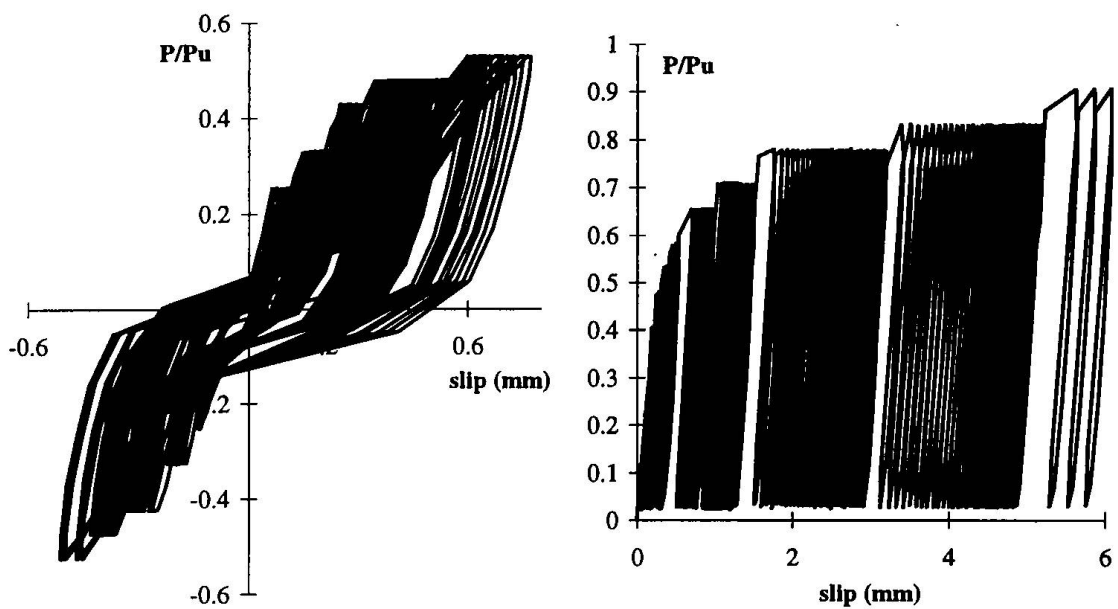


Fig. 2 Load versus slip plots for symmetric cyclic (test 15 - left) and unidirectional cyclic (test 13 - right) loading

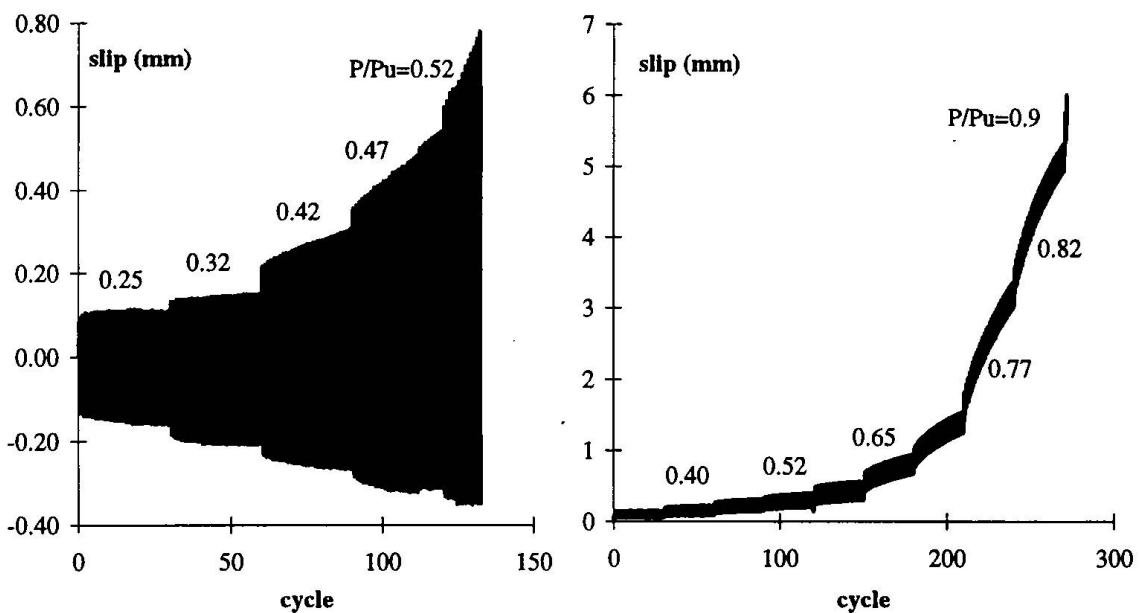


Fig. 3 Slip per cycle versus cycle plots for symmetric cyclic (test 15 - left) and unidirectional cyclic (test 13 - right) loading

Six specimens were tested under cyclic load, where the loading pattern involved complete reversal of the load. The time for one load cycle was typically three minutes. The rate of loading was increased as the load range increased in order to keep the cycle time constant. The load was applied for thirty cycles at each load level. A typical load-slip plot is presented in Figure 2 (test 15). From the figure it is clear that the slip incremented with every cycle, even at the lowest applied load level, however it is not immediately clear from the figure whether or not shakedown was achieved at the lowest applied load level. In order to obtain a better appreciation of the rate of increase of slip with load cycles, the data was presented as slip versus cycle number. Again, the data for test 15 is presented in Figure 3. It is clear from this figure that at a given load range the slip increases approximately linearly with cycles, and so it was possible to fit a straight line to the data within any given load range. This was repeated for every test, at every load range, for load in each direction. The slope of the straight line gives the slip growth per load cycle. This is presented in Figure 4 on a logarithmic scale.

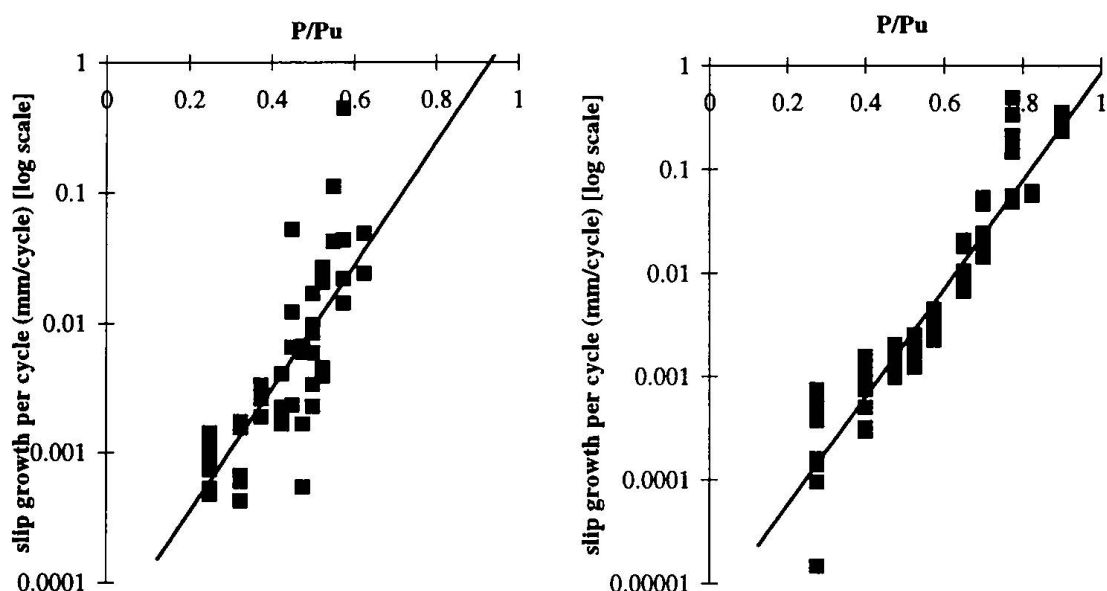


Fig. 4 Slip growth per cycle versus load plots for symmetric cyclic (test 15 - left) and unidirectional cyclic (test 13 - right) loading

3.3 Unidirectional cyclic test results

Three specimens were tested under cyclic load, where the load ranged from zero to maximum load. The time for one load cycle was typically one and a half minutes. A typical load-slip plot is presented in Figure 2 (test 13), the slip versus cycle number is plotted in Figure 3, and the slip growth per load cycle is presented in Figure 4 on a logarithmic scale.

3.4 Empirical relationship for the rate of slip growth

From the data presented in Figure 4, best fit lines were calculated to predict the slip growth per load cycle. This gave the following relationships:

symmetric cyclic load,

$$\log_{10}[\text{slip growth per cycle (mm/cycle)}] = -4.41 + [\text{peak load (kN)}] \times 0.0119 \quad \text{Eqn. 1}$$

unidirectional cyclic load,

$$\log_{10}[\text{slip growth per cycle (mm/cycle)}] = -5.29 + [\text{peak load (kN)}] \times 0.0130 \quad \text{Eqn. 2}$$

It is evident from figure 4 that symmetric cyclic loading leads to a faster growth of slip.

4. Conclusions

Incremental slip occurs in stud shear connectors under repeated loading, leading to incremental collapse of composite beams. Symmetric cyclic loading leads to a faster rate of slip growth than unidirectional cyclic loading. By using a push-out test adapted for cyclic loading, it is possible to obtain empirical equations for the rate of slip growth as a function of load. This information can be used by designers to estimate the rate at which incremental collapse will occur in composite beams under repeated loading.

5. References

- Chapman, J.C. *Composite construction in steel & concrete - the behaviour of composite beams*, Structural Engineer Vol 42 No 4 April 1964 pp 115-125
- Davies, C. *Small scale push-out tests on welded stud shear connectors*, Concrete Sept 1967 pp 311-315
- Davies, C. *Steel-concrete composite beams with flexible connectors: a survey of research*, Concrete Dec 1967 pp 425-430
- ENV 1994-1-1:1992 *Eurocode 4: Design of composite steel and concrete structures Part 1.1 General rules and rules for buildings*
- Gattesco, N. & Giuriani, E. *Experimental study on stud shear connectors subjected to cyclic loading*, Journal of Constructional Steel Research vol 38 No 1 1996 pp 1-21
- Goble, G.G. *Shear strength of thin flange composite specimens*, Engineering Journal AISC Vol 5 No 2 April 1968 pp 62-65
- Hallam, M.W. *The behaviour of stud shear connectors under repeated loading*, University of Sydney School of Civil Engineering Research Report R 281 August 1976
- Hawkins, N.M. & Mitchell, D. *Seismic response of composite shear connections*, Journal of Structural Engineering ASCE Vol 110 No 9 September 1984 pp 2120-2136
- Hawkins, N.M. *The strength of stud shear connectors*, Civil Engineering Transactions IEAust 1973 pp 46-52
- Johnson, R.P. & Oehlers, D.J. *Analysis and design for longitudinal shear in composite T-beams*, Proceedings ICE Pt 2 71 Dec 1981 pp 989-1021
- Maeda, Y. Matsui, S. & Hiragi, H. *Effects of concrete placing direction on static and fatigue strengths of stud shear connectors*, Technology Reports of the Osaka University Vol 33 No 1733 Oct 1983 pp 397-406
- Mainstone, R.J. & Menzies, J.B. *Shear connectors in steel-concrete composite beams for bridges, Part 1: Static and fatigue tests on push out specimens*, Concrete Sept 1967 pp 291-302
- Oehlers, D.J. & Carroll, M.A. *Simulation of composite beams subjected to traffic loads*, in "Composite construction in steel and concrete" C.D. Buckner & I.M. Viest ed 1987 pp 450-459
- Oehlers, D.J. & Coughlan, C.G. *The shear stiffness of stud shear connections in composite beams*, Journal of Constructional Steel Research 6 (1986) pp 273-284
- Ollgaard, J.G. Slutter, R.G. & Fisher, J.W. *Shear strength of stud connectors in lightweight and normal weight concrete*, Engineering Journal AISC April 1971 pp 55-64
- Thirugnanasundaralingam, K. *Continuous composite beams under moving loads*, PhD Thesis Monash University May 1991
- Viest, I.M. *Investigation of stud shear connectors for composite concrete and steel T-beams*, ACI Journal Vol 27 No. 8 April 1956 pp 875-891

Load-Slip Curve of Shear Connectors Evaluated by FEM Analysis

Christos KALFAS

Dr Civil Engineer
Democritus University of Thrace
Xanthi, Greece

C. Kalfas, born in 1947, has Univ. degrees in civil engineering and mathematics. His PhD thesis is in Composite Structures. Now, he is an Assist. Professor in the Metallic Structures Laboratory of D.U.T.H.

Petros PAVLIDIS

Civil Engineer
PhD Student
Xanthi, Greece

Petros Pavlidis, born in 1971, obtained his engineering degree in 1993, at the Democritus Univ. of Thrace. He is now in the final stage of the preparation of his PhD thesis on Composite Structures.

Summary

A new numerical method for the evaluation of the characteristics describing the mechanical behaviour of the shear connection in composite structures, is proposed. The method is based on F.E.M. and takes into account linear and non linear behaviour of the materials. The reliability of the method is proved by comparison with experimental results.

1. Introduction

From the very beginning of the application of composite structures many investigators have been concerned with the behaviour of the shear connection between concrete slab and steel beam. Many different types of shear connectors have been developed and investigated all over the world. Among them the most preferable are the headed studs and for the determination of their mechanical behaviour a number of papers has been published. In these works the experimental procedure of the push out test is mostly used in order to obtain the full load-slip curve, the failure load and the up-lift between slab and beam. Although this procedure has been established as the basic method for the design of composite elements, it has some disadvantages as time and money costs and need of specialized laboratories.

Due to the complexity of the three dimensional stress and strain state, no mathematical modeling of the push out test has been appeared. So, there are not closed analytical solutions of this problem and the only available formulas for the calculation of the parameters affected the behaviour of the shear connection, are based on the statistical evaluation of test results.

In our days Finite Elements Method (F.E.M.) can be used to solve such problems. This is the basic idea for the development of a new numerical method based on F.E.M. which is described in the current paper. The three parts consisted a composite section are simulated with different types of standard Finite Elements (F.E.) which can be found in the library of any F.E. package. The model is then analyzed taking into account linear and non linear behaviour of the materials and introducing the appropriate yield criteria. According to this procedure all the characteristics of the shear connection are determined.

The results of the proposed method were compared with experimental data in order to prove the reliability of the method. Experimental results obtained from series of push-out tests performed in

the Steel Structures Laboratory of the Democritus University of Thrace (D.U.T.H.), according to the push out test procedure of EC4 [1].

2. Numerical model and analysis

In the developing of the proposed method the basic idea is the modeling of the concrete slab, the steel beam and the shear connector of a push-out test specimen by different types of finite elements. In the beginning a simple model had been investigated taking into account the linear behaviour of the materials [7] and the reliability of that model had been proved by comparison with experimental results from Nakajima and Abe[8]. The same model was used for a new series of push out tests which were performed in the Steel Structures laboratory of D.U.T.H. according to the procedure and full instructions giving in EC4. The experimental results were more accurate with the F.E. model of the new specimen [6].

In the present paper, a modified F.E. model taking into account the inelastic behaviour of the materials, is studied. Each of the three parts of the composite section has been modeled by different elements. The concrete slab is modeled by non linear volume elements, the steel beam by a rigid bar element and the shear connectors by non linear beam elements. All these elements are offered as standard ones in all commonly used F.E. packages. In our case COSMOS/M program is used. The F.E.M. discretization of the push out test, as it is appeared in the F.E.M. program, is shown in Fig. 1.

The concrete slab is divided into 48 elements along X-direction, 40 elements along Y-direction and 5 elements along Z-direction. For the steel beam only one element is needed due to the high stiffness of the used element. Each of the shear connectors, is divided into 4 elements along the Z-direction. The resulted aspect ratio of the volume elements is 1:1:1.6, which satisfies the limits for these aspect ratios [3].

Only the half of the push out arrangement is modeled, due to the symmetry and the solution time. For the application of the support conditions all nodes at X1 and X2 surfaces (Fig. 1) are restricted to move in Y-direction as these surfaces resist in the compression load. All nodes along

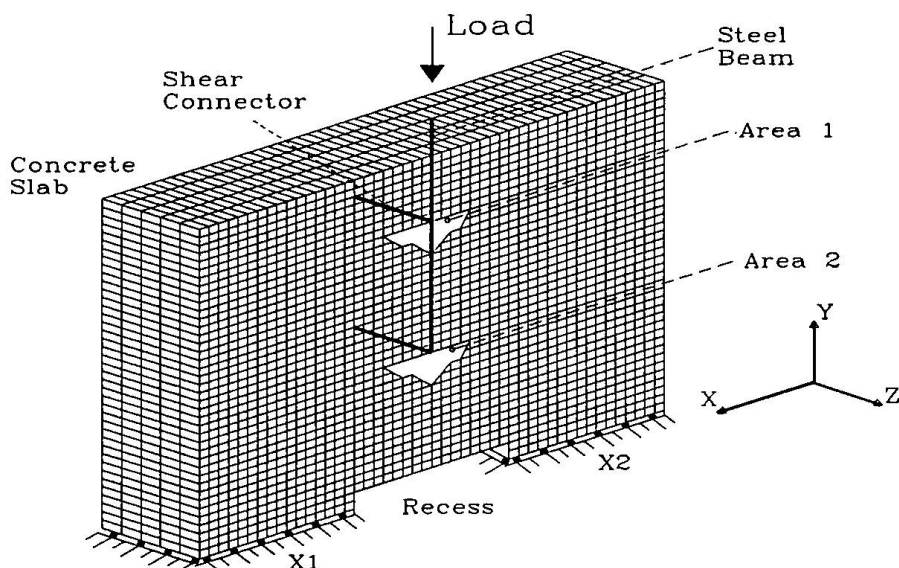


Fig. 1 Discretization of the push out test

the rigid bar element, which model the steel beam, are restricted to move in Z-direction due to the symmetry. A basic observation refers to the separation of the concrete behind the shear connector even when the loading is low [4,10]. According to this observation, a double grid of nodes towards the shear connectors (in Z-direction) is created producing volume concrete elements. The concrete nodes in front of the studs are merged with the nodes of the beam elements representing the studs (Fig. 1 - Area 1 & 2). The concrete nodes of the second grid behind the studs, are not merged with the nodes of the beam elements due to the detachment of the concrete. This assumption eliminates additional stiffness actually added in the area behind the studs. For each material of the composite section, appropriate yield criterion is considered. The Huber-von Misses model is used to simulate the behaviour of the shear connector material. For this model the yield criterion can be written in the form :

$$F = \sqrt{3} \bar{\sigma} - \sigma_y = 0$$

where : $\bar{\sigma}$: the effective stress
 σ_y : the yield stress

For the concrete two models are introduced, the Drucker-Pracker and the Huber-von Misses model. In Fig. 5 the load-slip curves obtained by both models, are compared with experimental data. As it seems, better results are obtained by the Drucker-Pracker model, for which the behaviour and the failure load are more close to the experimental data. For this reason the last model is preferred. In this case the yield criterion can be written in the form :

$$F = 3\alpha\sigma_M - \sigma_y + k = 0$$

where : σ_M : the mean stress
 σ_y : the effective stress
 α, k : material parameters

For the solution of the above F.E. problem the Newton-Raphson iterative method is used. A solution is reached when the difference between external and internal forces approaches zero. At each iteration, displacements are modified to minimize this difference. The COSMOS/M program is used in the non linear mode analysis.

In Fig. 2 the stress concentration is shown when the loading is applied to the model. Concentration of stresses is occurred at the surfaces X1, X2 (Fig. 1) and in the area in front of the stud connectors. Experiment verifies that concentration, by the crushed concrete area.

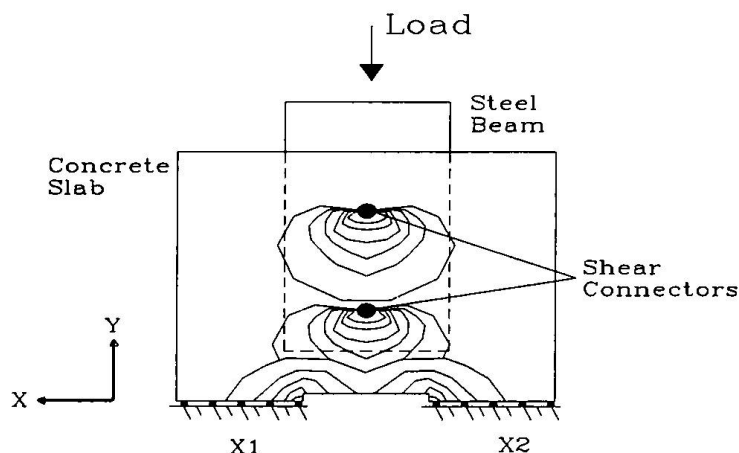


Fig. 2 Stress concentration when the loading is applied.

3. EXPERIMENTAL WORK

All the experimental work has been carried out in the Steel Structures Laboratory of the Democritus University of Thrace (D.U.T.H.). Two categories of tests were performed. The first category is concerned with the determination of the mechanical behaviour of the materials used in the preparation of the push-out specimen. Such tests were performed according to EC2 [2] and EC3 specifications for the materials of the concrete slab and shear connector, respectively. In the second category a series of push-out tests were prepared and performed according to EC4 [1] specifications.

For the concrete, cube specimens, 15x15x15 mm, were tested according to EC2 [2]. The mean compressive strength at 28 days was found 21.4 N/mm^2 . The elastic modulus of the concrete is calculated according to the procedure proposed by EC2 and the strain-stress diagram is shown in Fig. 4. For the material of the stud connectors, tension test has been performed according to the procedure proposed by EC3. The idealized stress-strain diagram of the stud connectors is shown in Fig. 3. No tests for the material of the steel beam have been made, because the beam is deliberately very rigid in comparison with the other two elements, so a high stiffness element was introduced for which no additional information is needed.

Each push-out specimen consists of an HE 260 B steel beam of total length 600 mm, two concrete slabs attached to the flanges of the steel beam with dimensions 500x600x100 mm for each slab, and stud connectors with a shank of 13 mm in diameter and 75 mm in height. A short recess of 200 mm wide and 3-4 mm height is formed to the concrete slabs. The natural bond at the interface between the steel flange and the concrete is prevented by greasing the steel flanges before casting the slab. During the execution of the test, the slip between the steel beam and the concrete slabs is measured by four electronic deflectometers, which are placed at the top surface of the slab in different points to ensure the accuracy of the overall test. All the data from the gauges and the load cell are registered electronically into the computer for further elaboration. The mode of failure in all the cases was the shearing off, just above the weld collar of the connectors. A very small uplift separation was observed.

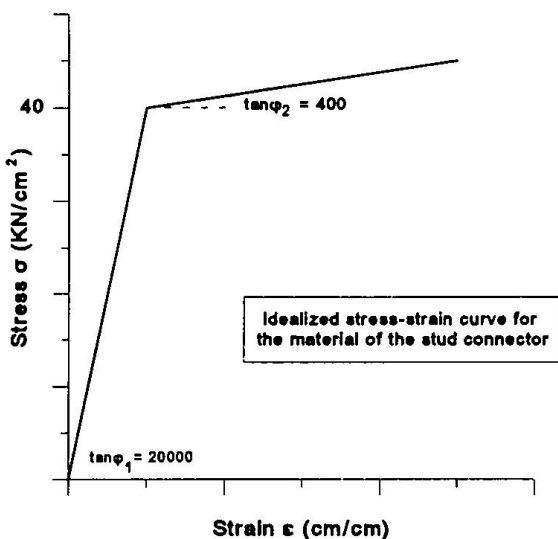


Fig. 3 Stress-Strain diagram for the of the shear stud connector.

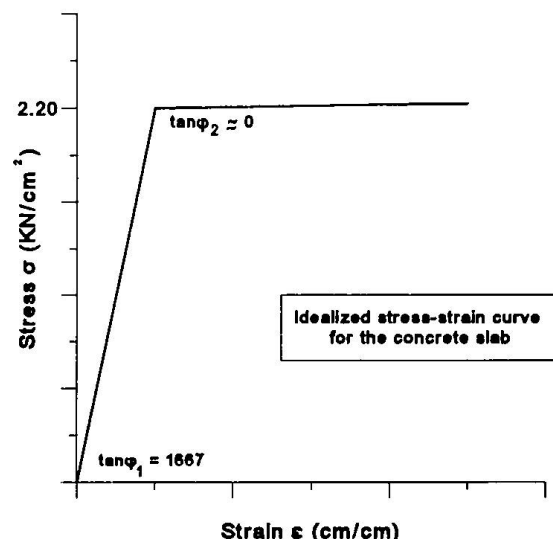


Fig. 4 Stress-Strain diagram for the concrete slab.

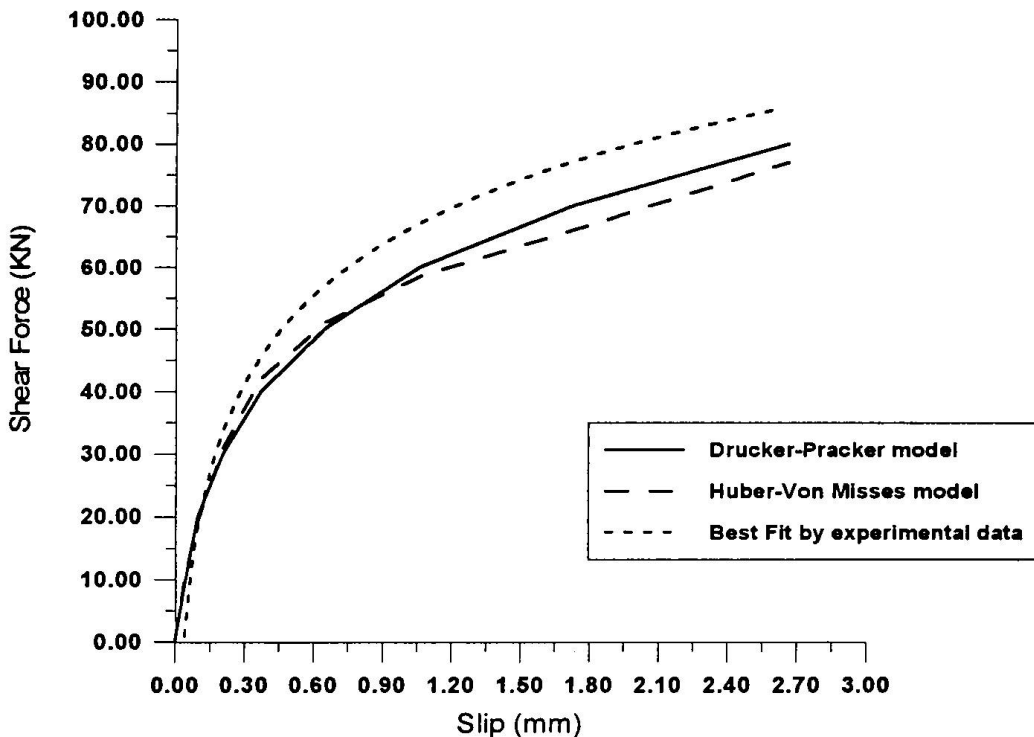


Fig. 5 Comparison of experimental data and F.E.M. analysis results

4. COMPARISON OF RESULTS

The comparison between experimental and numerical results, is shown in a slip-shear force plot (Fig. 5). Values of the shear force per stud are on the vertical axis and the corresponding average slip values are on the horizontal one. The upper dashed curve represents the best fitted line to the measurements of the push-out tests described in the previous paragraph. The other two curves have been obtained by the F.E.M. analysis of the present model. The continuous line represents the results of the analysis when the Drucker-Pracker yield criterion is used for the concrete, and the lower curve has been plotted for the results obtained by using the Huber-Von Misses model. As it is shown from the diagram the results of the F.E.M. analysis are in a good agreement with the experimental ones and always on the safety side. The Drucker-Pracker curve approaches the curve of the experimental data more closely. The deviation is very small when the load is low and becomes greater for higher values of the load. The maximum deviation between the experimental and the F.E.M. analysis (Drucker-Pracker model) results is about 14%, which is acceptable for the case.

The deviation appears to have greater values in the region corresponding to intermediate values of loading. There is only a slight deviation at the point of failure. The mean value of the failure load calculated from the test measurements, is 84 KN. The corresponding values taken by the present method are 80 KN and 77 KN for the Drucker-Pracker and the Huber-Von Misses model, respectively.

5. CONCLUSIONS

A simple method based on the finite element techniques has been developed to simulate and analyze the push out arrangement. Appropriate yield criteria are used for the materials. The numerical results are close to the experimental ones and on the safety side. The method is reliable for the elastic, which is restricted, and inelastic area.

The advantage of the present method is that the method permits a prediction of the behaviour of the shear connection and the stud. Since all the numerical results are conservative, but still close to the experimental ones, the proposed method can be used substituting or together with the experimental procedure cover cases such test procedures are a great percentage of the overall cost in money and time. Also, this method is useful in cases of lack of specialized laboratories needed for the performance of push out tests.

REFERENCES

1. EC-4, ENV 1994-1, Design of composite steel and concrete structures, 1992.
2. EC-2, ENV 1992-1-1, Design of concrete structures, 1992.
3. Horst, Werkle, 1995, *Finite Elemente in der Baustatik*, Vieweg Verlag.
4. Jayas, B.S. & Hosain, M.U., 1987, *Behaviour of Headed Studs in Composite Beams : Push-out Tests*, Civil Engrs, vol.15, pp 240-253.
5. Kalfas, C. & Pavlidis, P. & Tzourmakliotou, D. 1994, *Finite element simulation and analysis of steel-concrete composite structures*, Proceedings of the 4th ASCCS International Conference, Kocise, Slovakia, pp 548-551.
6. Kalfas, C. & Pavlidis, P. & Galoussis, E. & Liolios, A., 1995, *A F.E.M. Evaluation of Push Tests for Shear Connectors*, Proceedings of the Eurosteel 1995, May 18-20, Athens, Greece.
7. Kalfas, C. & Pavlidis, P. & Galoussis, 1995, *An Approach to simulate the Push out Tests*, Proceedings of the Nordic Stell Construction Conference, June 19-21, Malmo, Sweden.
8. Nakajima, A. & Abe, H., 1994, *Experimental Study on Behaviour of Horizontal Shear of Composite Girder*, Proceedings of the 4th ASCCS International Conference, Kocise, Slovakia, pp 348-351.
9. Narayanan, R., 1988, *Steel-Concrete Composite Structures - Stability and Strength*, Elsevier Applied Science Publishers Ltd.
10. Yam, C.P., 1981, *Design of Composite Steel-Concrete Structures*, Surrey University Press.

The Load-Bearing Capacity of Steel-HPC Composite Beams

Sandra BULLO

Architect
Univ. Inst. of Arch.
Venice, Italy

Sandra Bullo, born in 1963, graduated in architecture in Venice, subsequently specialising in R.C. structures at the Milan Polytechnic. Her main research interests are in steel-concrete composite structures and in creep effects in non-homogeneous structures.

Roberto DI MARCO

Associate Professor
Univ. Inst. of Arch.
Venice, Italy

Roberto Di Marco, born 1948, is Associate Professor of Civil Engineering. At present he is carrying out research on non-linear analysis of R.C. structures, on the use of new materials in civil engineering.

Summary

As far as steel-concrete composite beams are concerned, the use of high performance concrete (HPC) gives rise to an increased stiffness in the shear connectors and a reduction in ultimate slipping.

A numerical simulation referring to simply supported beams demonstrates that, at least in the case of full interaction, the brittle behaviour of the connection does not significantly affect the load-bearing capacity of the structure because flexural failure of the midspan section due to rupture of the materials occurs before any shear failure of the connection due to its capacity for deformation being exceeded.

1. Introduction

The mechanical characteristics of high performance concrete (HPC) lead to a variation in the behaviour of the beam-slab system, relating to two distinct factors:

- a variation in the behaviour of the cross section because of the greater strength and stiffness of the concrete forming the slab;
- a marked change in the behaviour of the shear connectors between the two elements.

Experimental tests on stud connectors, forming part of a research program being developed at the University Institute of Architecture in Venice, have shown that, as the strength of the concrete increases, there is an increase in both the strength and the stiffness of the connection, while there is a significant reduction in its ductility /1/.

It is therefore essential to investigate the effects that the brittle behaviour of the connector may have on the behaviour of the beams - be it in the case of a full connection or of a partial connection - because if the slip requirement is greater than the slip capacity of the connectors, then shear failure will occur before the ultimate flexural load is reached.

A parametric investigation was developed, varying both the mechanical characteristics of the materials and the geometric dimensions of the cross sections, to assess ductility requirements in different conditions and identify any design rules.

2. Effects of the concrete's strength on the behaviour of the connector

Fig. 1 and Table 1 illustrate some of the results of the experimental trials that the authors performed on the behaviour of stud connectors by means of push-out tests on standard samples. Said results show that a higher-strength concrete coincides with an increase in strength and stiffness, but also with a reduction in the extent of slipping at failure (s_c) and at the maximum load (s_u).

R_{cm} (MPa)	P_{max} (kN)	s_u (mm)	s_c (mm)
32.50	109.16	5.597	7.865 (*)
59.55	153.00	4.398	6.023 (*)
94.40	191.82	3.538	3.740

(*) slipping measured when P has fallen to $0.95 \cdot P_{max}$)

Table 1 Average experimental values for maximum loads and slipping of Nelson connectors (R_{cm} =mean cubic compressive strength, shank diameter $\phi=19$ mm).

3. Numerical Model

The study assessed the load-bearing capacity of simply supported composite beams, with uniformly distributed load, considering both the behaviour of the HPC and the load-slip relationships that can reproduce the behaviour of shear connectors in HPC.

Since the problem is far from linear, an incremental procedure till the collapse was used: at each step, the solution was found using an iterative process on the cross sections discretized in strips and along the axis of the beam divided into short lengths dx .

The model assumed the linearity of the strains in the steel beam and slab cross sections (indexes s and c , respectively) (Fig. 1) and any effects of the lifting of the slab were disregarded in view of their scarce influence on the slipping value emerging from the study /2/.

Having assumed the sectional deformations (the strain $\varepsilon_{os}(x)$ of the top fiber of the steel part; the curvature $\chi(x)$ common to the two elements; and the relative slipping $s(x)$) as unknown quantities, the conditions of equilibrium were established. In view of the presence of slipping, the equilibrium condition for the shear stresses at the beam-slab interface was added to the usual equilibrium conditions for the translation and rotation of the section.

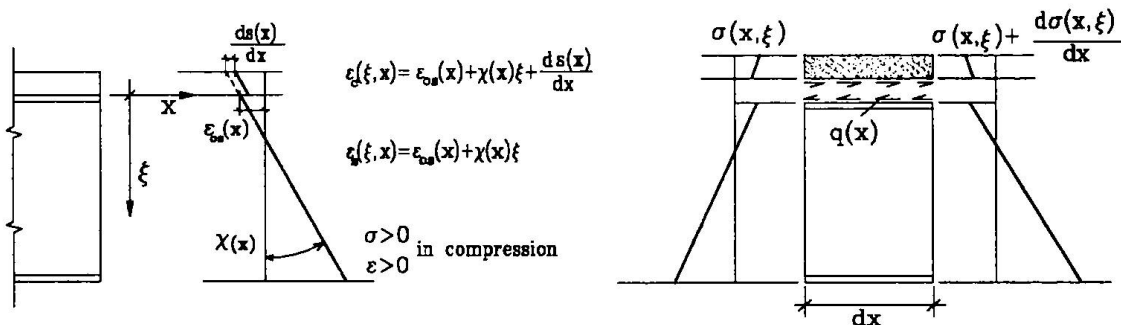


Fig. 1 Deformation in the section and beam length dx .

Taking a secant linear formulation for the constitutive laws into account, the system for finding the solution took shape as follows:

$$\begin{aligned}
 \varepsilon_{os}(x)[EA] + \chi(x)[ES] + \frac{ds(x)}{dx}[EA]_c &= 0 \\
 \varepsilon_{os}(x)[ES] + \chi(x)[EI] + \frac{ds(x)}{dx}[ES]_c - M(x) &= 0 \\
 \frac{d\varepsilon_{os}(x)}{dx} \frac{1}{[EA]_s} + \frac{d\chi(x)}{dx} \frac{1}{[ES]_s} - q(x) &= 0
 \end{aligned} \tag{1}$$

where:

- $[EA]$, $[ES]$, $[EI]$, $[EA]_c$, $[ES]_c$ are the stiffness coefficients of the whole section and of the slab, depending on the state of deformation across the secant modulus of the materials $E_{c,sec}$ and $E_{s,sec}$;

- $\overline{[EA]}_s$, $\overline{[ES]}_s$ are the stiffness coefficients of the steel section, depending on the variation in the deformation in dx , across the secant modulus relating to said variation ($\overline{E}_{s,sec} = d\sigma/d\varepsilon$);

- $q(x)$ is the shear action per unit of length coming to bear on the connector ($q(x) = R_{sec} s(x)$); R_{sec} is the secant stiffness of the connector per unit of length).

The finite differences method was used, applying backward integration, to solve the differential equations comprising system (1).

Once the boundary conditions had been established ($\varepsilon_{os}(x=0)=0$; $\chi(x=0)=0$; $s(x=L/2)=0$), the solution was obtained by applying the shooting technique, i.e. having assigned an arbitrary value to $s(x=0)$, system (1) was then solved for the subsequent sections up to the midspan. The procedure was iterated, updating $s(x=0)$, until the condition $s(x=L/2)=0$ was satisfied.

4. Numerical analysis

The analysis was performed in order to emphasize the extent of the maximum slip requirement in relation to changes in the following parameters:

- the reaction of the connector and slab to changes in the strength of the concrete;
- the span of the composite beam;
- the arrangement of the connectors along the beam.

4.1. Properties of the materials

The following constitutive laws were used:

- for the steel: elasto-plastic strain-hardening law, with the strain-hardening amounting to 100 MPa;
- for the concrete: the non-linear laws proposed in the Model Code 1990 with crushing strain $\varepsilon_{cu} = 0.0038$ and, in the case of HPC, in the Recommended Extension to the Model Code /3/, with crushing strain $\varepsilon_{cu} = 0.0030$.

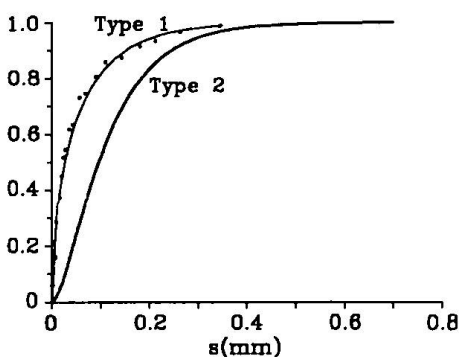
4.2. Properties and arrangement of the connectors

The load-slip law of the connector was modeled by means of the exponential relationship proposed by Ollgaard /4/, and already used in /2/, /5/, /6/, /7/, /8/:

$$P = P_u (1 - e^{-\beta s})^\alpha$$

where: $\alpha = 1.7$, $\beta = 1.15 \text{ mm}^{-1}$, $s_c = 7.0 \text{ mm}$ for the type 1 curves (studs in ordinary concrete)

$\alpha = 0.5$, $\beta = 1.10 \text{ mm}^{-1}$, $s_c = 3.5 \text{ mm}$ for the type 1 curves (studs in HPC) (Fig. 2)



having obtained the values of the coefficients α e β from an analysis of the results reported in the literature (for the type 1 curve) /9/ or from a fitting operation on experimental findings obtained by the authors (for the type 2 curve) /1/.

Two solutions were considered for the distribution of the connectors along the beam:

- evenly distributed (arrangement type A);
- evenly distributed at intervals, following the distribution of the shear stresses under a constant load (arrangement type B).

Fig. 2 Load-slipping relationships

4.3. Numerical tests

The investigation considered beams characterized by the cross sections illustrated in Fig. 3, with spans of 15, 25, 30 and 40 m, mean cylindrical concrete strengths of 35 and 80 MPa, and connectors having the constitutive laws of Fig. 2, according to the following table.

CODE	NC1-15	NC2-15	NC1-25	HP2-15	HP2-25	NC1-30	NC1-40	HP2-30	HP2-40
f_{cm} (MPa)	35	35	35	80	80	35	35	80	80
P-s	Type 1	Type 2	Type 1	Type 2	Type 2	Type 1	Type 1	Type 2	Type 2
Span L (m)	15	15	25	15	25	30	40	30	40
L/H	13.0	13.0	21.5	13.0	21.5	13.3	17.8	13.3	17.8

Table 2 Characteristics of beams for numerical tests

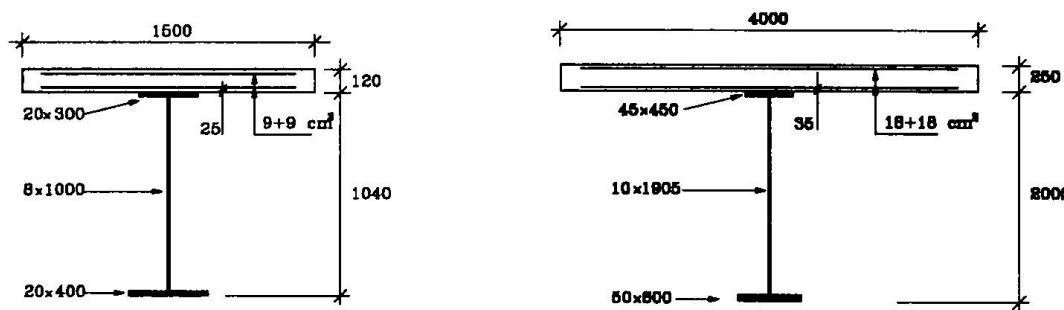


Fig. 3 Cross sections of beams for numerical tests

The maximum global strength of the connectors (Q_d) for the creation of the full shear connection was established by means of an elasto-plastic analysis of the cross section with no slipping.

4.4. Numerical test results

For each of the cases considered, the most significant results are given in Table 3.

CODE	NC1-15	NC2-15	NC1-25	HP2-15	HP2-25	NC1-30	NC1-40	HP2-30	HP2-40
$M_{max,sez}$ (kN*m)	4830.8	4830.8	4830.8	5113.3	5113.3	30225.0	30225.0	31645.0	31645.0
$M_{max}/M_{max,sez}$	0.9933	0.9957	0.995	0.986	0.987	0.987	0.989	0.991	0.988
$slip_{max}$ (mm)	3.275	2.583	4.095	1.651	1.841	3.196	3.367	2.563	2.717
$slip_{max}/s_u$	0.468	0.738	0.585	0.470	0.525	0.457	0.481	0.732	0.776

Table 3 Numerical test results

These data show that, assuming a perfect interaction between the two materials ($\varepsilon_c = \varepsilon_s$), the load-bearing capacity of the beam (M_{max}) is always lower than might be expected on the basis of the flexural strength of its midspan cross section ($M_{max,sez}$).

In fact, the increase in the load applied, and consequently in the acting moment, coincides with an increase in the rate of slipping $ds/dx = \varepsilon_c - \varepsilon_s$ (curves a and b, Fig. 5, for the two types of concrete) and this leads to a reduction in the values of both the maximum resisting moment and the ultimate moment (curves c and d for the ordinary concretes, and f and g for the HPC, Fig. 5). The maximum load that the beam can withstand is the load at which the acting moment at the midspan cross section reaches the same value as the resisting moment, with the corresponding value of the parameter ds/dx ; further loading is impossible because it would induce a corresponding increment in the acting moment and in ds/dx , and hence a reduction in the resisting moment.

New equilibrium conditions beyond the maximum load condition can only be achieved by reducing the actions, and the branch of the loading curve up to failure due to the maximum strength threshold being reached becomes unstable.

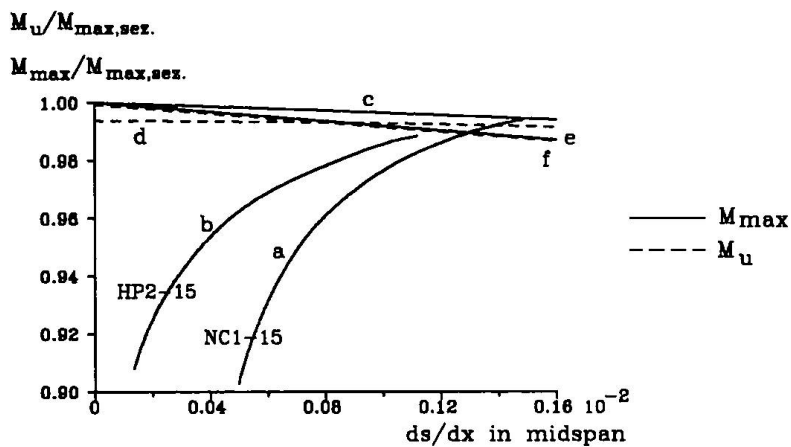


Fig. 4 M_{max} and M_u with changing values of ds/dx

The reduction in resisting capacity with ds/dx becomes more obvious in the case of HPC slabs. Moreover, the greater stiffness of the slab and connection - due to the higher strength of the concrete - gives rise to a reduction in the maximum slipping at failure, so the reduction in load-bearing capacity remains proportionally almost independent of the type of concrete, and the ductility of the connectors (though lower than in the case of ordinary concretes) is sufficient to prevent brittle failure of the beam due to rupture at the connection (Table 3 compares the findings for NC1-15, NC2-15, HP2-15).

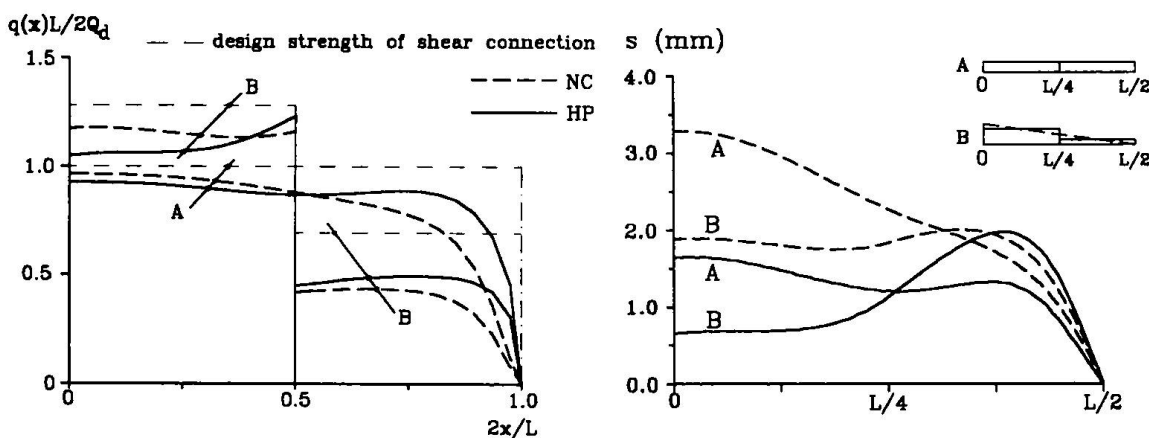


Fig. 5 Shear stresses and slipping along the connection for beams NC1-15 and HP2-15, and for stud connector arrangements A and B.

Fig. 5 shows the distributions of the theoretical resisting actions of the connector (which are uniform in case A, whereas they are twice as great in the supporting area as in the middle of the beam in case B) and the distributions of the actual stud reactions when the maximum load-bearing capacity is reached.

From a comparison of the diagrams, it is clear that the design conditions, based on the assumption of a full plasticization of the connector, coincide substantially with the actual situation in both types of concrete.

The beam-stud-slab system therefore seems, even in the case of HPC, to allow for a redistribution of the stresses, having a generally ductile behavior instead of the brittle behavior detected in the connector alone.

The two distributions consequently prove virtually equivalent in terms of load-bearing capacity, but the same cannot be said for the slipping requirement. The diagram in Fig. 5 shows that, in the case of ordinary concrete, the type B arrangement of the connectors leads to a more uniform distribution of slipping than with the type A arrangement, also reducing the maximum slipping value; in the case of HPC, on the other hand, the uneven distribution of the slipping phenomena is accentuated and their maximum value, which is reached nearly the middle of the beam, is greater than in the case of the uniform (type A) connector arrangement.

6. Conclusions

This study has shows that the behaviour at failure of composite beams made with HPC is influenced not only by changes in the behaviour of the connection, but also by the interaction of the latter with the resistant and deformative reaction of the slab.

In the cases considered here, the ultimate load coincided with flexural failure, thanks also to the contribution of the HPC slab towards reducing the slip requirement.

The study has also demonstrated that the arrangement of the connection is of little significance for the purposes of flexural failure, whereas the arrangements considered were far from comparable in terms of any failure occurring due to the ultimate slipping threshold being exceeded, so special attention must be paid to the identification of the ideal arrangement of the connectors.

References

1. S. BULLO, R. DI MARCO: "Effects of high-performance concrete on stud shear connector behavior", Proceedings of Nordic Steel Construction Conference, Malmö, Sweden, June 1995, pp. 577-584.
2. J. M. ALIBERT, K. ABDEL AZIZ: "Calcul des poutres mixtes jusqu'à l'état ultime avec un effet de soulèvement à l'interface acier-béton", Construction Métallique, n°. 4, 1985, pp.3-36.
3. CEB: Bulletin d'Information n. 228 "High performance concrete - Recommended extensions to the Model Code 90", July 1995.
4. J. G. OLLGAARD, R. G. SLUTTER, J. W. FISHER: "Shear strength of stud connectors in lightweight and normal-density concrete", Engrg. J. Am. Inst. Steel Constr., vol. 8, April 1971, pp. 55-64.
5. J. M. ALIBERT, A. G. LABIB: "Modèle de calcul élasto-plastique de poutres mixtes à connexion partielle", Construction Métallique n°. 4, 1982, pp. 3-51.
6. J. M. ALIBERT: "Etude critique par voie numérique de la méthode proposée dans l'Eurocode 4 pour le dimensionnement des poutres mixtes acier-béton à connexion partielle", Construction Métallique, n.1, 1988, pp. 3-26.
7. R. P. JOHNSON, N. MOLENSTRA: "Partial shear connection in composite beams for buildings", Proc. Instn. Civ. Engrs., Part 2, vol. 91, Dec. 1991, pp. 679-704.
8. S. BULLO, R. DI MARCO: "Influenza della limitata capacità di scorrimento della connessione sulla portanza di travi miste realizzate con calcestruzzi ad alte prestazioni", C.T.E., Napoli, 7-9 November 1996, pp. 21-30.
9. D. J. OEHLERS, C. G. COUGHLAN: "The shear stiffness of stud shear connectors in composite beams", Journal of Construct. Steel Research, n.6, 1986, pp.273-284.
10. D. J. OEHLERS, G. SVED: "Composite beams with limited-slip-capacity shear connectors", Journal of Structural Engineering, Vol. 121, No. 6, June 1995, pp. 932-938.
11. EUROCODE N.4: "Design of composite steel and concrete structures", Part 1-1: General rules and rules for buildings, ENV 1994-1-1, October 1992.

Design of Shear Transfer in Concrete-Concrete Composite Structures

Fritz MÜNGER

Civil Engineer

Hilti AG, Schaan

Principality of Liechtenstein

Fritz Münger, born in 1944, graduated with a degree in civil engineering from the Swiss Fed. Inst. of Technology, Zurich in 1968. For 20 years he has worked in Switzerland and South Africa as a design engineer in industrial and bridge construction. Since 1989 he has been a project manager with Hilti Corporate Research.

Manfred WICKE

Professor

University of Innsbruck

Innsbruck, Austria

Manfred Wicke, born in 1933, has his civil engineering and Ph.D. degrees from Vienna Technical University. He worked in and later headed a design office of a firm, primarily involved in the design of buildings, bridges and power plants. Since 1971 he has been a full professor for concrete structures at Innsbruck University.

Norbert RANDL

Civil Engineer

University of Innsbruck

Innsbruck, Austria

Norbert Randl, born in 1967, graduated with a degree in civil engineering from the Innsbruck University. Since 1993 he has worked in the Institute for Concrete Structures at Innsbruck University.

Summary

For the design of concrete composite constructions, the transfer of internal stresses across the bond interface between new and old concrete is a critical aspect. A design method has been developed with the aid of specific tests for rough, sand-blasted and smooth surfaces. Test results known from literature have been taken into account. This new design approach considers cohesion, friction and the shear resistance of the reinforcement in determining the effective shear transfer. It has been found that, contrary to the usual design approach, the full yield strength of the reinforcement cannot be equated to the tension clamping force across the interface.

1. Introduction

Placing new concrete on older concrete is a routine task in construction. It occurs at every joint in concrete construction work. For some time now, placing overlays has gained in importance as a result of the more frequent strengthening of existing structures. In such cases, a loadbearing layer of new concrete (overlay), is placed on the existing concrete structure. This overlay is usually cast directly or placed as shotcrete. It functions to augment the flexural compression or flexural tension zones, depending on the placement.

One of the problems encountered is the transfer of internal stresses acting across the bond interface between the old and the new concrete. In this respect, knowledge is required of the resistance of the bond interface to tensile and compressive forces in any direction. Initially, stresses in the bond interface result from a combination of external loads and internal forces of constraint. It must be borne in mind that stresses due to shrinkage and temperature gradients in the new concrete typically reach their maximum at the perimeter of the overlay. The

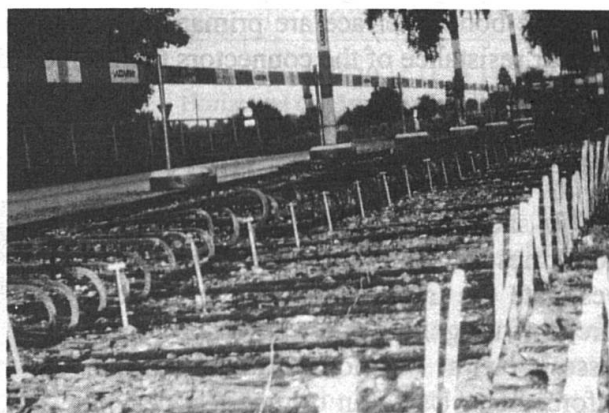


Fig. 1: Strengthening of a bridge

combination of external and internal stresses often exceeds the capacity of the initial bond, thus requiring the designer to allow for a debonded interface. This is particularly true in the case of bridge overlays which are subject to fatigue stresses resulting from traffic loads. Furthermore, these stresses are dependent on time, and bond failure can take place years after overlay placement.

2. State of the Art

Review of the literature reveals little research into the specific behavior of reinforced bond interfaces between new and old concrete. The majority of the existing studies concentrate on the transfer of shear forces across cracks [6]. The effect on the shear loading capacity of subsequent roughening the surface of the old concrete was first investigated in 1960 in the United States. A few years later, the so-called shear-friction theory was developed. This theory attempts to explain the phenomena with the aid of a simple saw-tooth model. According to this, the roughness of surfaces in the case of relative displacement always leads to a widening of the interface which sets up stresses in steel connectors passing across the interface. They, in turn, create clamping forces across the interface and thus also frictional forces. In the middle of the 1970's, further shear tests were conducted in New Zealand (Paulay [4]), in the United States (Mattock [5]) and in Germany (Daschner [7]).

In 1987, Tsoukantas and Tassios [8] presented analytical investigations into the shear resistance of connections between precast concrete components. They cover the different contributing mechanisms of friction and dowel action (fig. 2). In 1991/92, Menn [9], in Switzerland, looked into the behaviour of bond between old and new concrete using a series of beams which had been strengthened by additional reinforcement in a new layer of concrete placed on the underside of the beams. The results clearly demonstrated that a significant increase in loadbearing capacity can be achieved by proper roughening of the surfaces. If the surfaces are very rough, the steel connectors across the bond interface are primarily stressed in tension, whereas, if the surfaces are smooth, the shear resistance of the connectors themselves (dowel action) predominates.

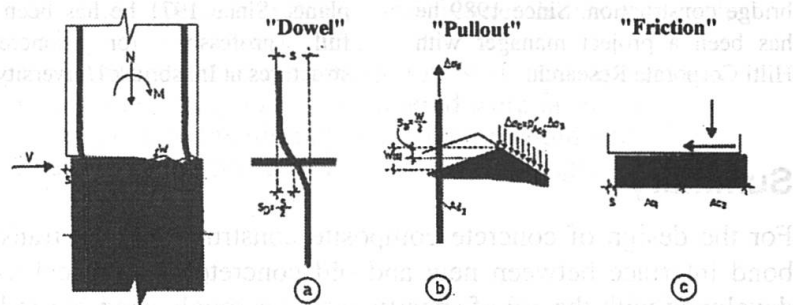


Fig. 2 Shear transfer in cracked concrete [8]

In 1991/92, Menn [9], in Switzerland, looked into the behaviour of bond between old and new concrete using a series of beams which had been strengthened by additional reinforcement in a new layer of concrete placed on the underside of the beams.

The results clearly demonstrated that a significant increase in loadbearing capacity can be achieved by proper roughening of the surfaces. If the surfaces are very rough, the steel connectors across the bond interface are primarily stressed in tension, whereas, if the surfaces are smooth, the shear resistance of the connectors themselves (dowel action) predominates.

3. Laboratory Tests by Hilti Corporate Research

Specific shear tests were carried out in the laboratories of Hilti corporate research to investigate the interrelationships of various degrees of roughness and transferable shear stresses with various amounts of reinforcement. Using an origine test design, it was possible to avoid any eccentric moments in the specimen and to allow for parallel separation of the interface surfaces (fig. 3). The roughened surfaces were treated with a de-bonding agent before the new concrete was placed.

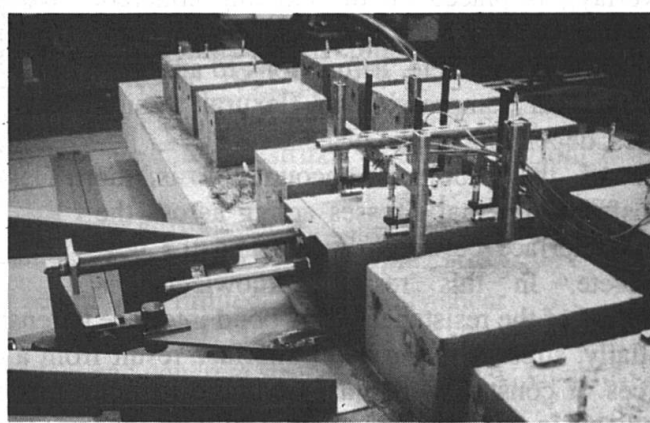


Fig. 3: Testing arrangement

The test results confirm the strong influence of roughness on shear resistance and shear stiffness. If the load-displacement curves are regarded in conjunction with the measured displacement, the three components of cohesion, friction and dowel action can be isolated and determined quantitatively. They make different contributions to the overall resistance (figs. 4, 5 and 6), depending on surface roughness and amount of reinforcement.

Hence, the frictional component predominates when the surface is blasted with a high-pressure water jet and larger amounts of reinforcement are provided. But small shear stresses can also be transferred even when no reinforcement is present, due to the good interlocking effect of the interface surfaces. In the case of sand-blasted surfaces, however, shear stresses are transferred by a combination of friction and dowel action, but the forces that can be resisted are generally far smaller than in the case of high-pressure water blasting.

It was also investigated whether the post installed rebar connectors are stressed to yield at ultimate shear transfer. For this purpose, the strain in the connectors at the level of the interface was measured. To avoid any disturbance of the bond, and in order to obtain the strain from tensile loading only, strain gauges were fixed in a central bore in the axis of the connectors.

These test results clearly show that, when surfaces have the above-mentioned degrees of roughness, the tensile force in the connectors does not reach the full tensile yield strength, contrary to assumptions for current design models. Tests carried out with connectors of various lengths confirm this result as they showed that reduced anchorage lengths are sufficient to carry the effective connector tensile force at maximum shear transfer capacity. Additional connector embedment (e. g., as required for theoretical connector tensile yield) did not result in increased shear transfer.

The loadbearing behaviour of smooth interface surfaces with connectors was also investigated. As displacement readings for the horizontal and vertical directions showed, there is in this case also a separation of the interface under shear loading and, thus, owing to the lack of roughness, a loss of contact between the shear surfaces. In this case, the entire resistance comes from dowel action.

On the basis of these findings, design approaches can now be developed which permit separate and realistic analyses of the various components of shear resistance. As a result, a standardised level of safety is ensured with respect to resistance, no matter whether the normal stresses at the interface are set up by an external normal force or internal connectors.

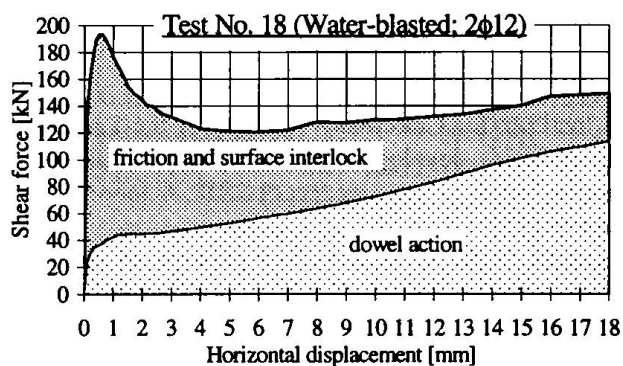


Fig. 4: Water-blasted surface

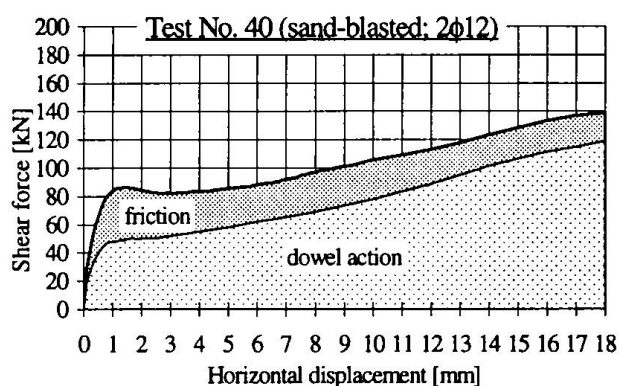


Fig. 5: Sand-blasted surface

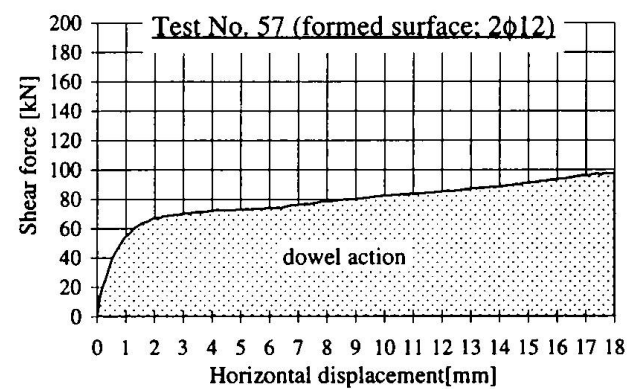


Fig. 6: Smooth surfaces

4. Design of Shear Transfer

4.1 Miscellaneous

The Institute for Concrete Structures of the University of Innsbruck, Austria, provided scientific support during development of this design method, which is based on EC2 [1]. The evaluation is contained in the thesis by Randl [10]. A more comprehensive description and examples can be found in [13].

Structures made of reinforced or prestressed concrete, which have a concrete overlay of at least 60 mm, may be designed as a monolithic building component if the shear forces acting in the interface between the new and the old concrete are resisted according to the following rules.

4.2. Loadbearing Capacity of Interface

Generally, an interface must be assumed to be cracked for design work. Connectors installed across the interface must be positioned in such a way that the shear force, V_{Rd} , between the new and the old concrete is transferred in the ultimate limit state.

$$V_{Rd} = \tau_{Rdj} \cdot b_j \cdot l_j \geq V_{Sd} \quad (1)$$

V_{Rd} Design value of interface shear force resistance

τ_{Rdj} Design value of the transferable interface shear stress in zone under review as per formula (2)

V_{Sd} Design value of interface shear force due to actions

b_j Width of interface in zone under review

l_j Length of interface in zone under review

The design value of transferable shear stress, τ_{Rdj} , can be calculated using formula (2) [10]. When doing so, the upper limit is given by the transferable compressive stress in the strut model for concrete:

$$\tau_{Rdj} = k_T \cdot \tau_{Rd} + \mu \cdot (\rho \cdot \kappa \cdot f_{yd} + \sigma_n) + \alpha \cdot \rho \cdot \sqrt{f_{yd} \cdot f_{cd}} \leq \beta \cdot v \cdot f_{cd} \quad (2)$$

cohesion friction dowel action compressive strut in concrete

τ_{Rd} basic value of design shear strength as per [1], section 4.3.2.3 (smaller value of new/old concrete)

$\rho = A_i / b_j l_j$ amount of reinforcement from connector in zone under review

k_T cohesion factor as per [13], table 1

$\sigma_n \leq 0,6 f_{cd}$ normal stress to external loads acting on the interface (compression positive)

μ coefficient of friction as per [13], table 1

f_{yd} design value of yield strength of connectors

α coefficient of dowel action as per [13], table 1

f_{cd} design value of cylinder compressive strength of concrete (smaller value of new and old concrete)

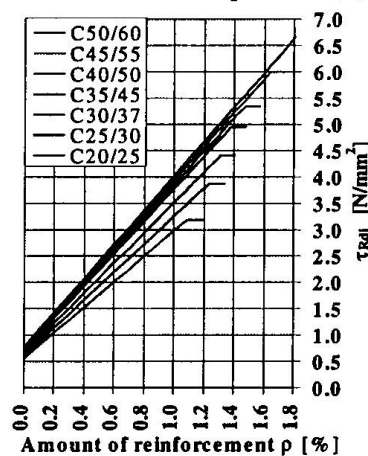
β coefficient as per [13], table 1

r mean roughness derived from sandpatching method (i.e. difference between peaks and valleys = 2r)

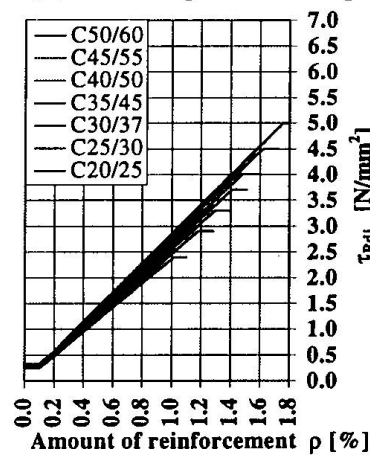
v coefficient as per [1] formula (4.20)

κ coefficient for tensile force in the connector as per [13], table 1

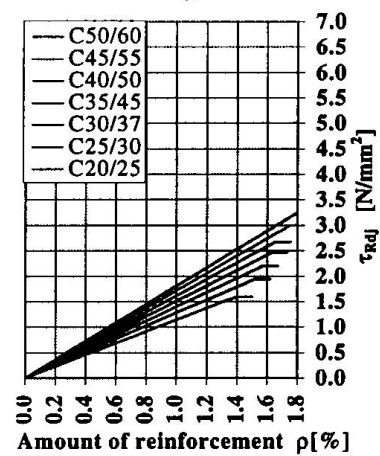
An evaluation of equations (1) and (3) for S500 grade steel is provided in the diagrams 1 to 3.



Dia 1: Water blasted surfaces



Dia 2: Sand-blasted surfaces



Dia 3: Smooth surfaces

4.3 Stressing of Interface

Normally, the design value of the interface shear force acting, V_{sd} , is determined from the flexural resistance of the cross-section. Consequently, bending is decisive for failure of the cross-section and reference is made to full connection, as in steel-concrete composite designs [2].

In the perimeter of the concrete overlay, the crack tensile force, F_{cr} , of the concrete overlay must be transferred in accordance with [1], section 4.4.2.2. Particular attention must then be given to transfer of the moment from the crack tensile force in order to avoid spalling effects.

4.4 Serviceability Limit State and Design Principles

For normal cases, where water blasting is used, the stiffness can be determined, at the strengthened cross-section assuming full composite action. Where sand-blasted or smooth interfaces are used, a reduction of the stiffness must be expected.

Variations in surface preparation for the same building component should only be allowed if resulting stiffnesses along the interface variations are compatible from a displacement standpoint. It must be noted here that interfaces with small shear stresses, without connectors according to section 4.3, may be assumed to be non-cracked for stiffness purposes.

The connectors must be adequately anchored in the old concrete and in the overlay. The actual tensile force, F_d , to be anchored may be taken as at least $F_d \geq 0.5 \cdot A_s \cdot f_{yd}$ when surfaces are rough or sand-blasted.

To shorten the anchorage length in concrete overlays, heads or plates can be provided. The concrete cone as well as the bearing stresses in the concrete below the anchoring component must be checked. The methods of calculation are given in [14].

When surfaces are smooth, shear dowels must be anchored at depths of at least 6 times the diameter in each case, or, better still, to avoid dowel pull-out at large displacements a value of 9 times the diameter is recommended.

5. Comparison with Literature

In his thesis [10], Randl has proven through a study of literature and with reference to worldwide research results that the determined design equations are conservative. The results are shown in figs. 7 and 8.

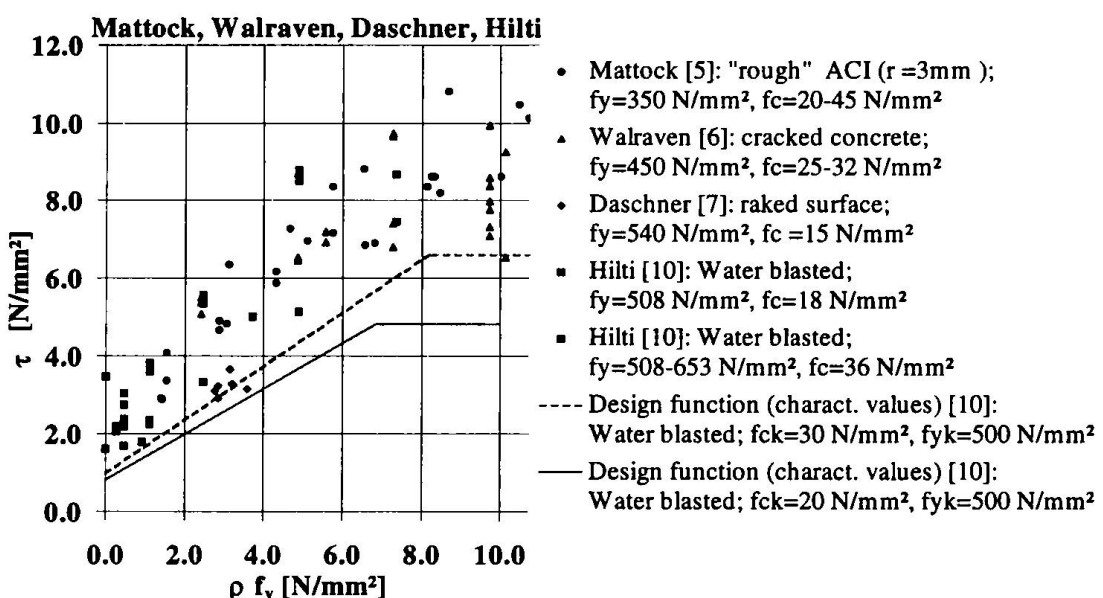


Fig. 7 Rough surfaces

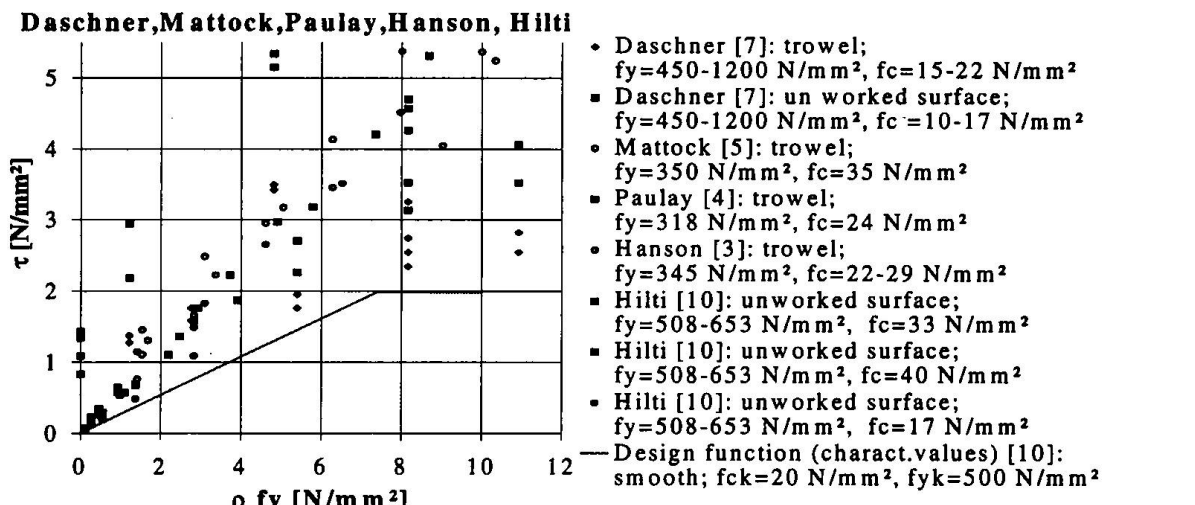


Fig. 8 Smooth surfaces

6. Summary

Contrary to design methods given in the literature, dowel resistance is considered along with cohesion and friction when determining shear resistance. With increasing roughness of surfaces, shear resistance and shear stiffness improve greatly. Furthermore, the distribution of total resistance shared by the three components changes considerably. The design method makes use of one single equation for calculating the resistance from the three components. In some cases, it is sufficient for the concrete overlay to be anchored at its perimeter.

This new design approach is particularly notable for its transparency. It is verified by the literature as well as by extensive testing conducted at Hilti Corporate Research. Through the use of design diagrams, the method can be made particularly straightforward for designers.

Literature

1. EC 2; Design of concrete structures: ENV 1992-1-1: 1991;
Part 1. General rules and rules for buildings
2. EC 4; Design of composite steel and concrete structures: ENV 1994-1-1: 1992;
Part 1-1. General rules and rules for buildings
3. Hanson, N.W.; Precast-Prestressed Concrete Bridges-. Horizontal Shear connections. Journal of the Portland Cement Association, Research and Development Laboratories, V.2, No.2, May 1960, pp.38-58
4. Paulay, T., Park, R. and Phillips, M.H.; Horizontal Construction Joints in Cast in Place Reinforced Concrete, ACI-Special Publication SP.42 Shear in Reinforced Concrete, 1974, Vol. II, 99. 599-616
5. Mattock, A. H.; Shear Transfer across an Interface between Concretes Cast at different Times, Structures & Mechanics Report SM76-3, University of Washington, Seattle, 1976, 68 pp.
6. Walraven J. C., Reinhardt H. W.; Theory and experiments on the mechanical behaviour of cracks in reinforced concrete subjected to shear loading. Heron Vol.26/1981.
7. Daschner, F.; Versuche zur notwendigen Schubbewehrung zwischen Betonfertigteilen und Ortbeton. Deutscher Ausschuss für Stahlbeton, H 372 Berlin, Ernst und Sohn, 1986
8. Tsoukantas S. G., Tassios T. P.; Shear Resistance of Connections between Reinforced Concrete Linear Precast Elements. ACI Journal, May-June 1989.
9. Menn, C.; Bonding of Old and New Concrete for Monolithic Behaviour
Swiss Federal Institute of Technology, Zürich. Report No. 185, 1991.
10. Rndl, N.; „Untersuchungen zur Kraftübertragung zwischen Neu- und Altbeton bei unterschiedlichen Fugenrauigkeiten“; Dissertation in Vorbereitung, Universität Innsbruck.
11. Hilti, Fastening Technology Manual, Rebar Fastening Guide B 2.2, 1994
12. Hilti, Fastening Technology Manual, Adhesive Anchors B 3.2, 1994
13. Hilti, Fastening Technology Manual, Rebar Fastening Guide for Overlays, B 2.3, 1997
14. CEB-Guide; On the Design of Fastenings in Concrete, Part 3, Draft March 95
Characteristic Resistance of Fastenings with Cast-in-Place Headed Anchors.

Connections for Timber-Concrete-Composite Structures

Hans J. BLASS

Professor of Civil Eng.
Universität Karlsruhe
Karlsruhe, Germany

Hans J. Blass, born 1955, received his civil engineering degree at Karlsruhe University in 1980. After four years in industry, he went back to Karlsruhe University and received his PhD. in 1987. From 1991 to 1995 he was professor for timber structures at Delft University of Technology and took his present position in 1995.

Marina SCHLAGER

Civil Engineer
Schöck Bauteile GmbH
Baden-Baden, Germany

Marina Schlager, born 1960, received her civil engineering degree at Karlsruhe University in 1988. She worked in structural timber research at Karlsruhe University until 1996 when she took her present position.

Summary

This paper presents information on the load-deformation behaviour and the manufacture of different types of timber-concrete connection. The failure modes of four different connections and their influence on the load-deformation behaviour and the failure modes of timber-concrete composite beams is outlined. The design of timber-concrete connections with dowel-type fasteners is summarised and the effect of load sharing between fasteners on the load-carrying capacity of the composite beam is emphasised.

1. Introduction

Timber-concrete-composite structures, used as bending members in floor systems, mostly consist of timber members in the tensile zone, a thin concrete layer in the compression zone and the connection between timber and concrete. The main advantages of this type of composite structure are:

- increased strength and stiffness compared to timber floors,
- improved sound insulation,
- increased fire resistance,
- easy method to reinforce existing timber floors.

The load-carrying behaviour of timber-concrete-composite structures is essentially influenced by the strength and stiffness of the connection between timber and concrete. This is valid for both, the short and long-term behaviour of the composite members. Apart from a large load-carrying capacity, connections for timber-concrete-composite structures should exhibit a high stiffness under service loads as well as distinct plastic deformations before failure. In addition, for economic reasons they should be easy to install.

2. Types of Connection

During a co-operative research project carried out at Delft University of Technology in the Netherlands and Karlsruhe University in Germany (Blaß et al. 1995), timber-concrete-composite structures with four different types of connection were studied:

- especially designed screws driven into the timber without pre-drilling under an angle of $\pm 45^\circ$,
- punched metal plate fasteners,
- grooved holes in timber beams filled with concrete and combined with a dowel, and
- grooved holes in laminated veneer lumber filled with concrete.

2.1 Screws

The screws used in the study were specifically developed for timber-concrete connections. They are driven into the timber without pre-drilling, resulting in low labour costs for the manufacture of the connections. Connections with different screw arrangements were investigated by Timmermann and Meierhofer (1993). Instead of placing the screw perpendicular to the joint between timber and concrete, they placed the screws under an angle of $\pm 45^\circ$, resulting in a truss-like loading of the connections, where the screws are loaded in tension and compression rather than in bending. This fact leads to a much stiffer connection compared to an arrangement perpendicular to the timber surface. The screw has two heads, the lower pressing the concrete formwork onto the timber beams. The upper head together with a part of the shank is encased in concrete.

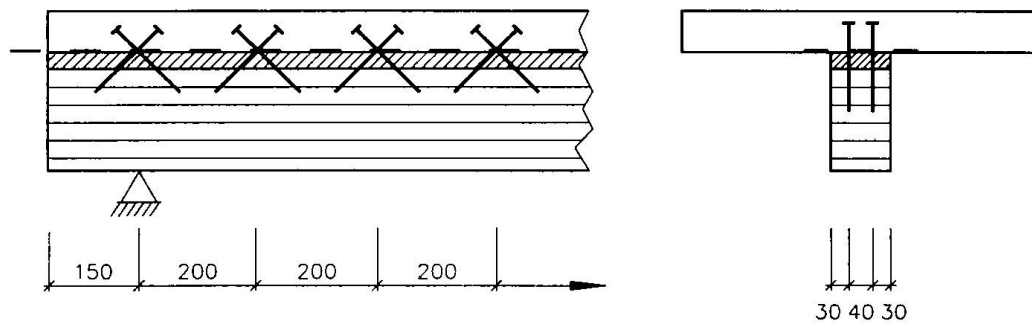


Fig. 1 Timber-concrete connection with crossed screws.

2.2 Punched metal plate fasteners

The punched metal plate fasteners, which are very common as connectors in timber trusses, were first bent about their longitudinal axis to form a right angle. The nails on the plate part later encased in the concrete layer were cut off in order to prevent voids in the concrete close to the plate. The other half was then pressed into the timber beam. This type of connection has to be prefabricated before shipping the beams to the building site.

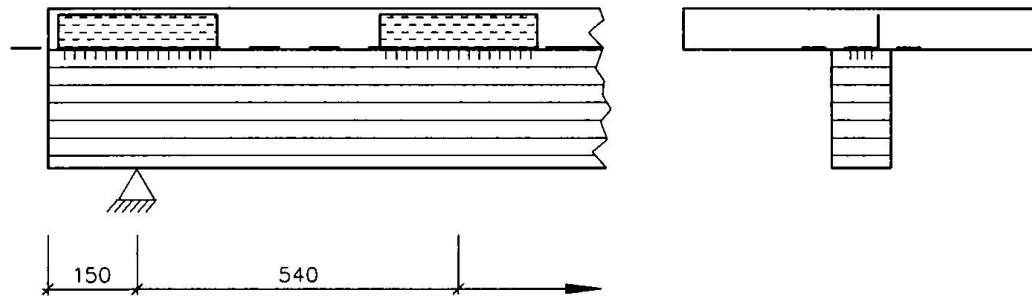


Fig. 2 Timber-concrete connection with punched metal plate fasteners

2.3 Grooved connections with dowels

In order to manufacture this type of cleat joint, first grooves with a diameter of 70 mm are routed 30 mm deep into the timber beam surface. Within this indentation, a hole with a diameter of 20 mm is drilled to take the steel dowel. The steel dowels - short pieces of concrete reinforcement bars - are then driven into the 20 mm holes. Concrete finally covers the upper part of the dowels and fills the remaining space in the grooves.

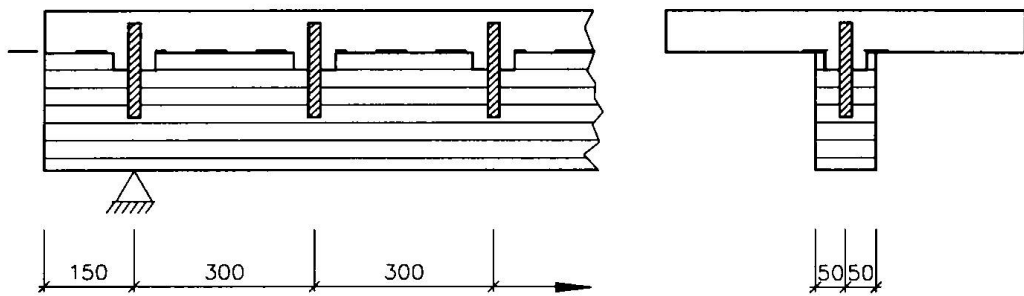


Fig. 3 Timber-concrete connection with grooved holes and dowels

2.4 Grooved connections in LVL

This type of timber-concrete connection is used for composite plate structures, where instead of timber beams laminated veneer lumber (LVL) as sheet material is used in the tensile zone. The joints are manufactured by grooving circular holes with a diameter of 115 mm and a depth of 15 mm into the LVL surface. The holes are conical in vertical direction in order to prevent a separation between timber and concrete. The concrete filling the flat holes forms a type of cleat which is able to transfer shear forces. In order to avoid a brittle failure of the concrete cleats, they are reinforced. The manufacture of the indentations is carried out with computer-controlled routing machines resulting in very economical connections.

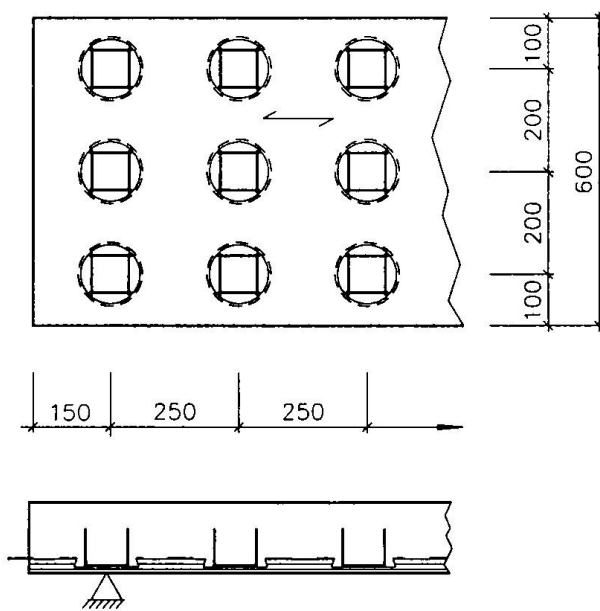


Fig. 4 Timber-concrete connection with grooved indentations in LVL

3. Load-Carrying Behaviour of Connections

In order to acquire sufficient data about the variation of the load-carrying behaviour, about 50 single shear specimens of every type of connection were tested in short-term tests. Although the failure modes of the four types were quite different, all types exhibited a high stiffness at service load level and distinct plastic deformations before failure.

Depending on the thickness of the intermediate layer between timber and concrete, the screws loaded in tension were either pulled out of the timber or failed in tension in the threaded part of the shank. After reaching the maximum load, the load on the connection decreased with increasing withdrawal of the screw (Figure 5 top left). The average maximum load for one pair of screws was about 18 kN at a displacement of about 1 mm.

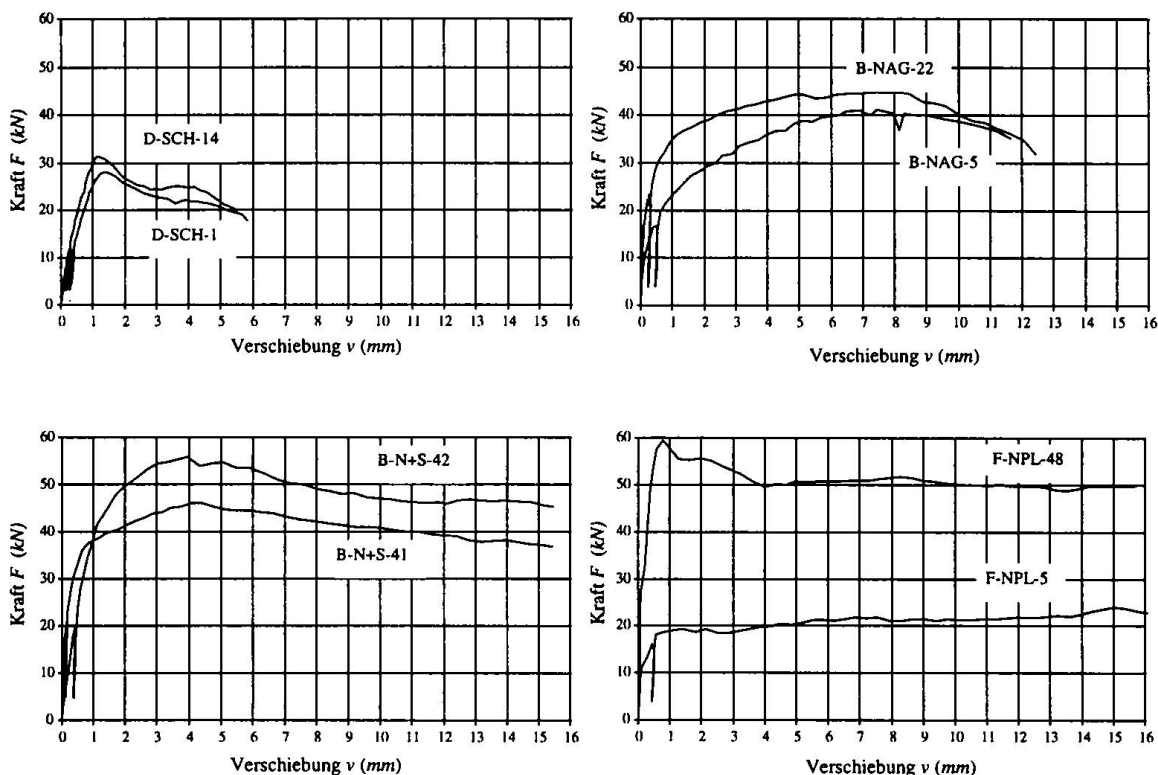


Fig. 5 Load-deformation-diagrams with maximum and minimum stiffness of four different connections. Screws (top left), punched metal plate fasteners (top right), grooved connections with dowels (bottom left), and grooved connections in LVL (bottom right)

The connections with punched metal plate fasteners failed due to bending and subsequent withdrawal of the punched out nails out of the timber. In some cases, nails failed in tension at the metal plate. The mean maximum load for one plate was about 48 kN, the stiffness modulus at service load level about 50 kN/mm.

Grooved connections exhibited a particular plastic deformation capability. The tests were stopped after a relative displacement of 15 mm between timber and concrete was reached. The failure for grooved connections with dowels was caused by dowel bending combined with concrete cracking in the vicinity of the dowel. The maximum load for one connector unit (indentation plus dowel) was about 50 kN, the stiffness modulus at service load level about 75 kN/mm. Grooved connections in LVL acted as large concrete connectors. In some cases, the load was still increasing when a displacement of 15 mm was reached. Failure was caused by reaching the embedding strength of the laminated veneer lumber. The average maximum load was about 50 kN per indentation, the corresponding stiffness modulus 120 kN/mm.

4. Load-carrying Behaviour of Timber-Concrete-Composite Beams

For each type of connection, ten timber-concrete composite beams were tested in short-term tests. For the composite beams with screws, punched metal plate fasteners and grooved connections with dowels, the span of the beams with a T-type cross-section was 5,40 m (Fig. 6 top), for the beams with grooved connections in LVL, the span was 4,50 m (Fig. 6 bottom).

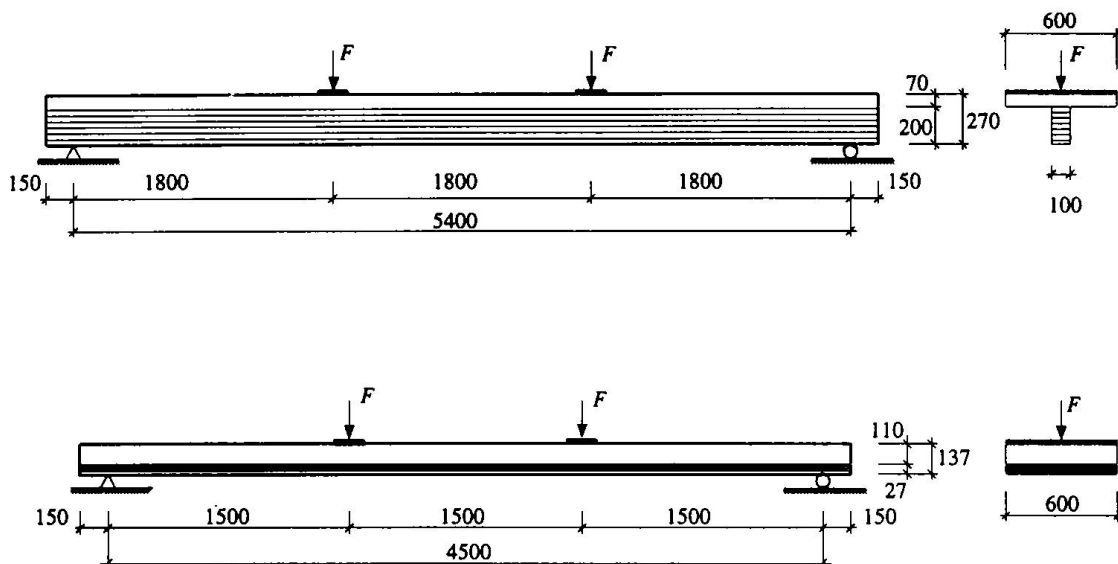


Fig. 6 Test specimens for timber-concrete composite beams. Connections are screws, punched metal plate fasteners, grooved connections with dowels (top), and grooved connections in LVL (bottom)

The influence of the connection behaviour on the load-deformation behaviour of the composite beams depends both on the load-carrying behaviour of the connections and on the load level of the connection loads before the failure of the beam. Since all four types of connection approximately exhibit an elastic-plastic load deformation behaviour, the load-deformation behaviour of the tested composite beams essentially depends on the load level of the fasteners. If the fasteners between timber and concrete govern the design, the highly loaded fasteners close to the supports will approach their load-carrying capacity, deform plastically and a certain amount of plastic deformation of the beams is to be expected before failure. If, on the other hand, the connection loads remain in the elastic range until the beam fails, the beams will basically behave linearly until failure.

Depending on the number and capacity of the connections, the behaviour of the tested beams ranged from linear-elastic until failure until elastic-plastic. The beams with the highest connection capacity (grooved connections in LVL) exhibited a linear load-deformation behaviour until failure. The brittle failure was caused by the failure of the LVL-layer under combined bending and tensile stresses.

The composite T-beams eventually all failed due to the combined bending/tensile failure of the timber beams. The composite beams with screws and those with grooved connections with dowels showed a pronounced plastic deformation before failure due to the plastic deformation in the timber-concrete connections. The failure of the connections close to the supports - withdrawal of the screws or splitting of the timber end cross-section and cracking of concrete, respectively - before the failure of the beams could be clearly observed in the tests. The beams with punched metal plate fasteners displayed a slightly curved load-deformation diagram, indicating the fact that the first connections approached their load-carrying capacity before the failure of the composite beam.

5. Design of Timber-Concrete Connections

Generally, the design of timber-concrete composite structures requires the consideration of the slip occurring in the joint between timber and concrete. A method for the calculation of the fastener loads for mechanically jointed beams or columns is e. g. given in Annex B and C of Eurocode 5 Part 1-1 (ENV 1995-1-1). The design of timber-concrete connections is dealt with in Eurocode 5 Part 2 - Design of timber structures - Part 2: Bridges. In many cases, the load-carrying capacity and the slip modulus of the connection have to be determined by tests. Testing is not required, however, for laterally loaded dowel-type fasteners inserted perpendicular to the shear plane. If there is no intermediate layer between timber and concrete, the strength of the joints with screws, dowels and threaded nails may be assumed 20 % higher than for corresponding timber-to-timber joints according to ENV 1995-1-1. The corresponding stiffness values may be taken 100 % higher than for corresponding timber-to-timber joints.

If the withdrawal strength and stiffness of screws or threaded nails is known, Eurocode 5 Part 2 also provides a method to design inclined fasteners for timber-concrete connections. The analytical model assumes a truss-like behaviour of the components, where for uni-directionally inclined fasteners the shear force is transferred by tensile forces in the fasteners and compression forces between timber and concrete, and for two-directionally inclined fasteners by tensile and compression forces in the fasteners.

If tests to determine the load-carrying capacity and the slip modulus of timber-concrete connections show a distinct plastic behaviour, a redistribution of loads from highly loaded fasteners to less loaded fasteners will occur in composite beams, as soon as the most stressed fasteners deform plastically. If the connection governs the design of the composite beam with a large number of fasteners, the characteristic load-carrying capacity of the beam therefore depends on the characteristic strength of a number of connections loaded in parallel, rather than on the characteristic strength of a single connection. This load-sharing increases the load-carrying capacity of the composite beam and should either be taken into account during the connection design or when determining the characteristic strength of timber-concrete connections.

6. References

Bajolet, D., Gehri, E., König, J., Kreuzinger, H., Larsen, H.J., Mäkipuro, R., and Mettem, C. (1997). PrENV 1995-2. Eurocode 5 - Design of timber structures - Part 2: Bridges.

Blaß, H.J., Ehlbeck, J., Van der Linden, M.L.R. and Schlager, M. (1995). Trag- und Verformungsverhalten von Holz-Beton-Verbundkonstruktionen. Forschungsbericht der Versuchsanstalt für Stahl, Holz und Steine, Abteilung Ingenieurholzbau der Universität Fridericiana Karlsruhe, 74 pp.

European Committee for Standardization (1993). ENV 1995-1-1. Eurocode 5 - Design of timber structures - Part 1-1: General rules and rules for buildings.

Timmermann, K. and Meierhofer, U.A. (1993). Holz/Beton-Verbundkonstruktionen. Forschungs- und Arbeitsberichte EMPA-Abt. Holz, Nr. 115/30, 87 pp.

Concepts and Details of Mixed Timber-Concrete Structures

Julius NATTERER

Professor

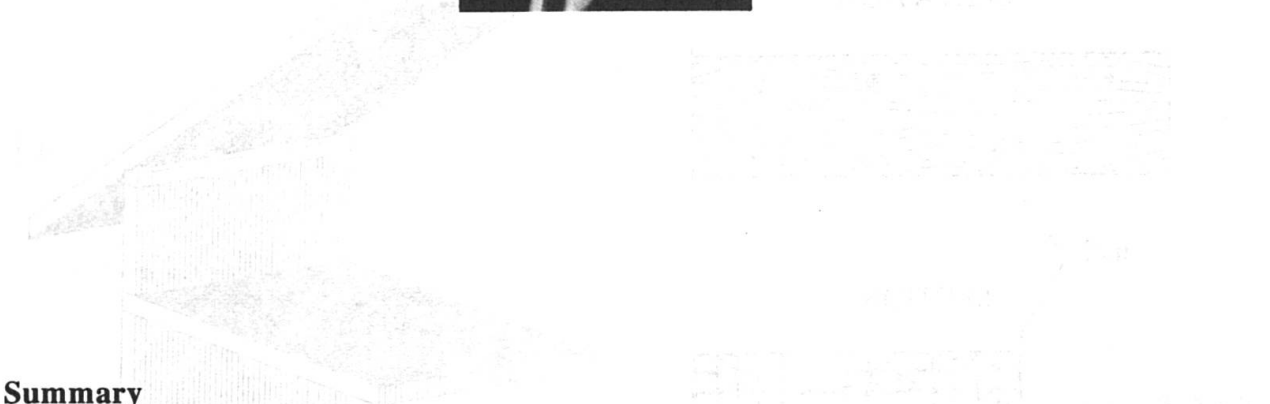
Swiss Fed. Inst. of Technology
Lausanne, Switzerland



Julius Natterer, born 1938.

In 1970, he founds his own office specialized in timber construction first in Munich, then in 1983, in Switzerland.

In 1978, he is named director of the Chair of Timber Construction of the Swiss Federal Institute of Technology in Lausanne. He is the author of several publications in timber engineering.



Summary

Buildings can be erected using timber in the floor in order to be more economical and lighter than conventional concrete constructions. For a span of three to six meters, timber floors made of vertical nailed planks are built. For a span of seven to fifteen meters, this kind of timber floor is connected to a concrete deck and becomes a composite wood-concrete system. In this case, the shear strength is taken by a groove in timber filled with concrete. The timber part can be made of planks, roundwood, glued laminated timber, regarding the expected aspect of the ceiling.

1. Introduction

Given the constant decrease in energy resources and the new consideration of environmental parameters, a way for an increasing use of wood in the construction is open. But the wood construction should not remain sectarian. In order to be economical, it must work together with other materials, traditionally used in construction. In the history of timber construction, there have always been composite constructions – timber frameworks with glue or mortar, walls of stone and bricks – the most lasting ones were in timber architecture. Examples from China and Japan to Frank and Alsacian framework constructions are well known. Essential criteria are a better behavior of the whole construction during a fire, as well as acoustics and vibration properties.

Today, quality criteria – fire, acoustics, vibration – are easily fulfilled through new shape applications, i.e. massive nail laminated floors and wood-concrete composite systems for wide-span and load supporting structures. Nail-laminated decks and wood-concrete decks including a load-bearing concrete slab present new advantages, especially for houses, schools and public buildings. Thanks to these techniques, the steadiness and bending properties of structures with minor dead loads can be economically fulfilled. Fire resistance times of 30, 60 or 90 minutes, as well as phonic insulation criteria up to 60 dB for walls and decks can be reached. The use of timber as construction material is the only way to save the world's forests. Timber use is directly linked to forest conservation and the planting of new trees.

The material selection is no proof for "good architecture". It is, however, an important contribution to the environmental conservation, even if it needs more concentration on the planning phase.

2. Vertical Nailed Planks

The system of vertical nailed planks has been one of the new techniques developed for several years at the Chair of Timber Construction at the Swiss Federal Institute of Technology, in Lausanne (EPFL). Several projects have been realized within the last years with this new method. This technique certainly matches to the requirements of modern constructions. The system is made of planks which are vertically nailed to each other (figure 1) and resulting into a plane surface.

These elements may be used without concrete for structural purposes, such as supporting walls, floors (ceilings) and sloping roofs (figure 2). Depending on the broad requirements, the planks may be either kept as raw material or painted, or covered with wall paper, or

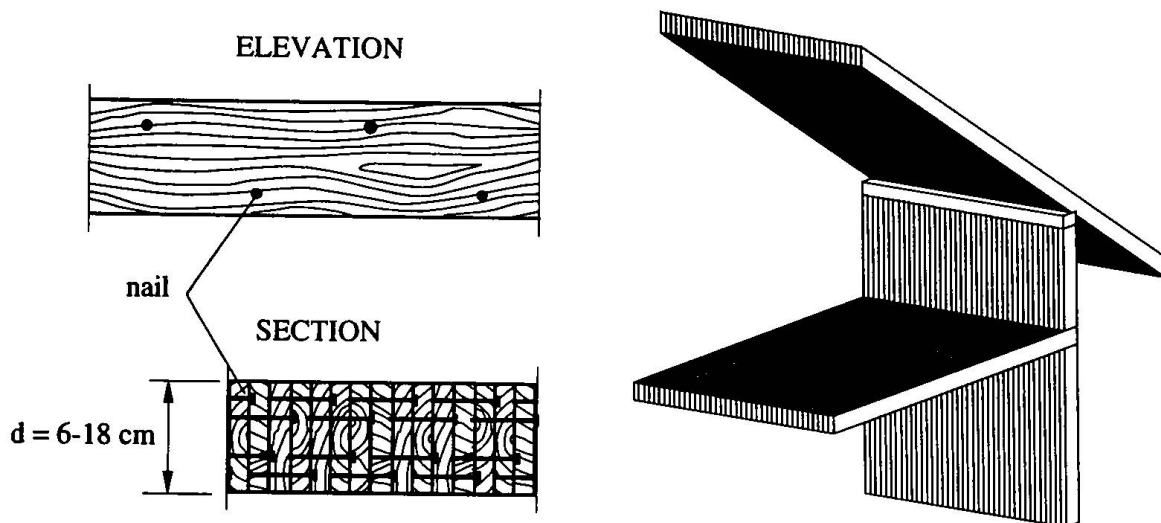


Fig. 1 - Nailing pattern for element construction.

Fig. 2 - Construction in vertical nailed planks.

anything else. High acoustical demands may be satisfied with the manufacture of special profiles, as shown in Figure 3 for ceiling elements. Various solutions which do not require the use of special tools are available to manufacture noise absorbers. For instance, a few millimeters shift of one out of two planks may be enough for the purpose aimed at. Architectural needs may also be a factor which be considered when proposing solutions.

Figure 4 shows three solutions out of many others which are available for floors made out of vertical nailed planks; acoustic insulation may be required, so as impact noise reduction or higher thermal inertia for the system. There are plenty of solutions and we must keep in mind that they may be directly used with this new support, provided that they are set up with respect to the wood material.

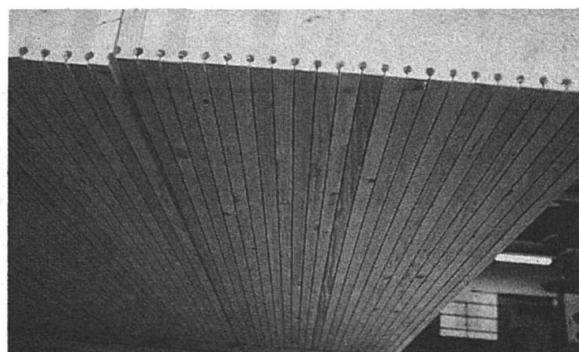


Fig. 3 - Prefabricated vertical-nailed planks elements with an acoustic profile.

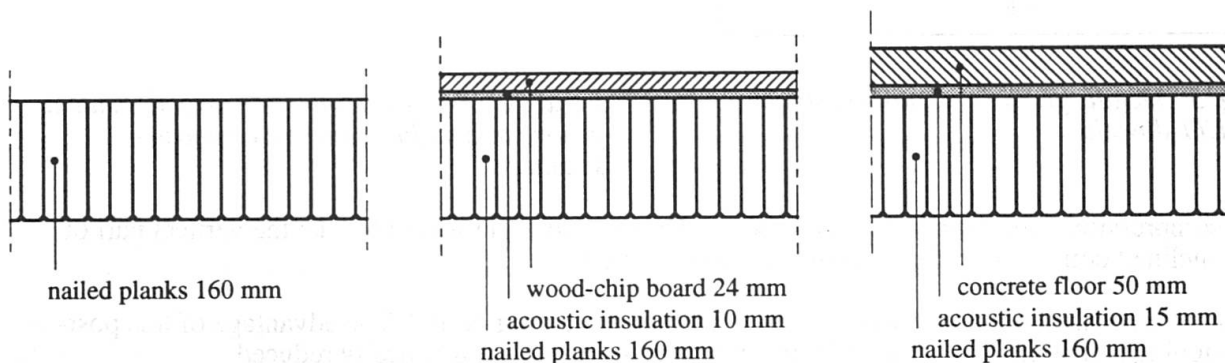


Fig. 4 - Examples of vertical nailed planks floor with different cover layers depending on specific requirements.

3. The Technique of Composite Structure

The timber-concrete composite structure is a system where the shuttering is directly included into the bearing part of the system. In this configuration, timber elements are covered by concrete, so that each component will efficiently work: timber in tension and concrete in compression.

In order to use the composite structure with high performances, it is important that concrete and timber are linked together with a connection as rigid as possible. In this case, the link between the two components is done with a system of grooves in the wood and post-tensioned dowels (figure 5).

The tests have shown that the link between the two materials does not depend on the rigidity of the link, but only on the position and the repartition of the grows. With this consideration, the efficacy of the liaison can be taken from 85 to 90 % of the composite effect.

Calculations for designing simply supported beams (and unidirectional slabs) are based on a simplified method taking into account the mechanical properties of both materials and the elastic behavior of the composite structure. Hypotheses have been made about the load distribution (uniformly distributed live load) and the real behavior of the groove-dowel detail.

The behavior of the groove-dowel detail is based on the push-rod model used in reinforced concrete beams. The shear forces are transmitted from the concrete to the wood

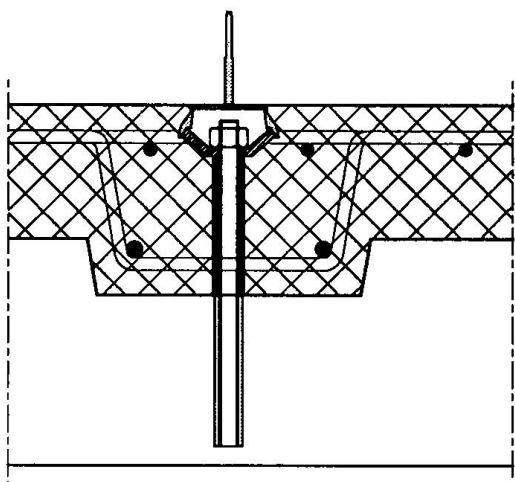


Fig. 5 - Detail: groove and post-tensioned Hilti-dowels

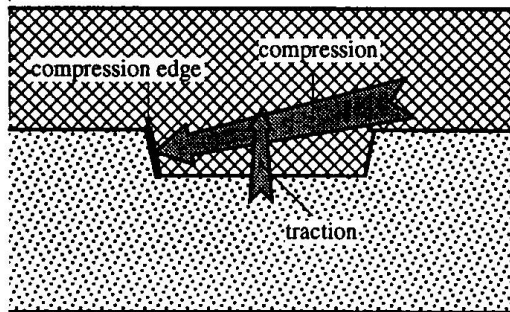


Figure 6 - Forces acting on the wood inside a groove in a timber-concrete composite structure.

by compression on the surface of the grooves. Dowels work in traction to take the vertical part of the inclined compression force on the grooves (figure 6).

Moreover, dowels are post-tensioned after the concrete curing period. The advantage of this post-tensioning is that the gap - caused by the concrete shrinkage - is drastically reduced.

One can introduce some rebars inside the grooves, perpendicularly to the planks direction. This solution will improve the transverse distribution of the load on the slab. Apart from this optional reinforcement, a low diameter reinforcement mesh is advised in concrete to reduce and redistribute curing cracks over the surface of the concrete.

Because of the parallel system created by the nailed planks (see figures 1 and 2), low quality timber can be used with reevaluated properties. As a matter of fact, one single low quality plank has a social behavior once it is connected with other planks and it is no more necessary to design such elements with the quality of the lowest plank. Hence, designing becomes also more efficient and less expensive in materials.

Figure 7 shows the groove and dowel distribution for a simply supported beam. They are concentrated near the supports, under assumption of a distributed load, in order to take internal shear forces with efficiency. Several constructions have already been erected using this new connection detail. Vertical nailed planks are often used for the tension part of the

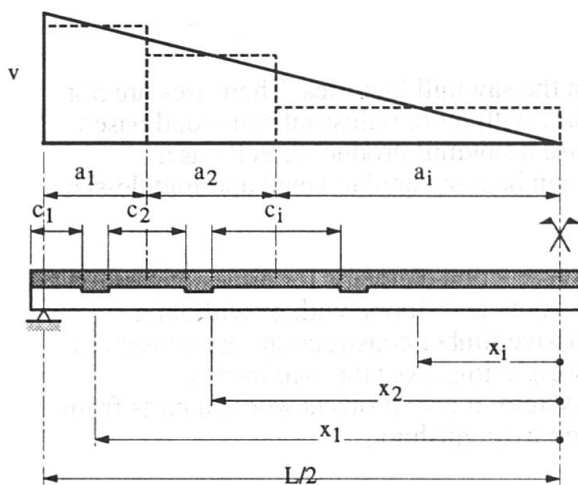


Fig. 7 - Groove positioning according to the shear force diagram.

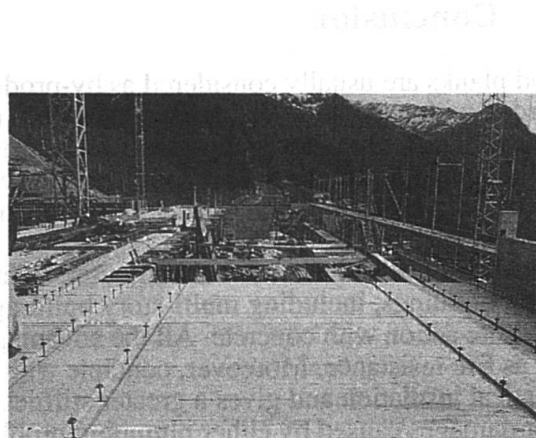


Fig. 8 - Wood elements and dowels for a timber-concrete composite slab: School in Triesenberg (FL).

composite structure in housing (figure 8), but we can also use round posts or glue laminated elements for longer span or higher load solicitations, like for bridges or industrial buildings.

Today's experience shows that this kind of system is still at a developing stage, but it is enough advanced to be applied in different ways. Composite timber-concrete systems show a great flexibility in their application. This technique has both the usual advantage of timber structure and the advantage of concrete structure. Figure 9 shows the behavior of three different floors submitted to the same live load, with regards to the dead load and the acoustical insulation.

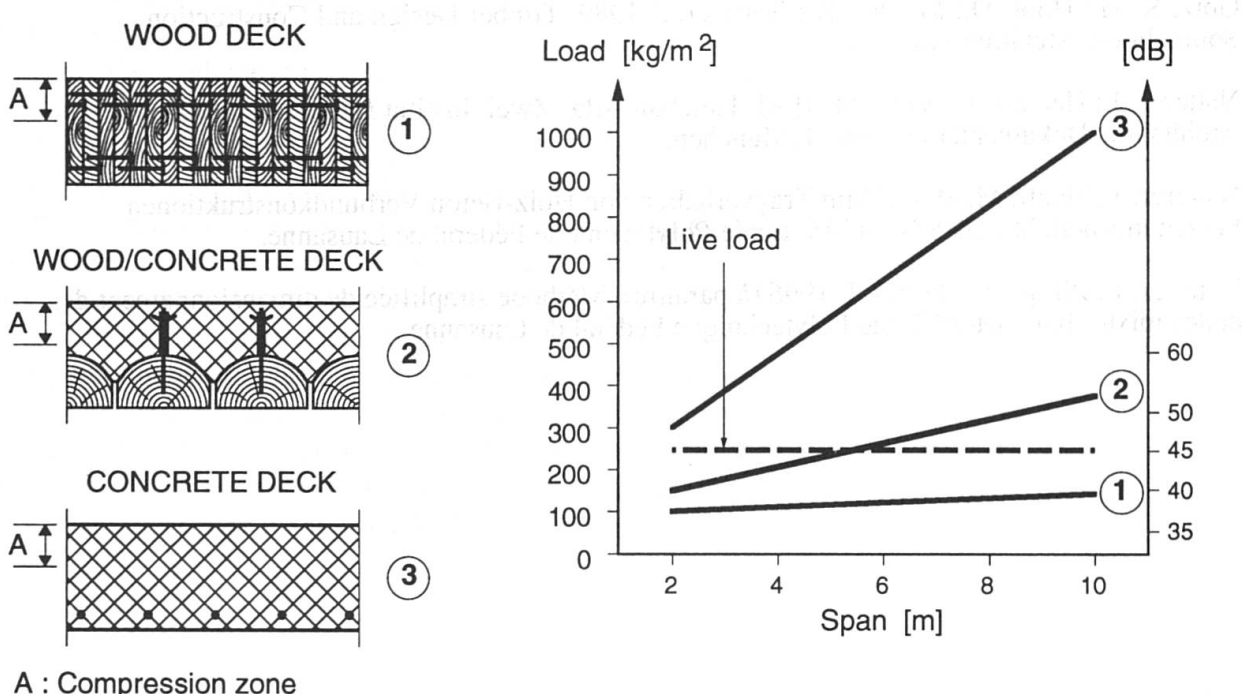


Fig. 9 - Behavior comparison of different floors.

4. Conclusion

Wood planks are usually considered as by-products from the sawmill factories. Their uses are not regarded with interest by engineers who would rather work with more industrialized wood based products. This paper shows an interesting alternative to use a sawmill product directly as a building material. It is worth noticing that this technique can be transferred to small and middle-size industries without too much financial investment.

Vertical nail planks have been already used as massive construction elements for different parts of several buildings, including multi-story buildings; walls, roofs and floors, with or without a composite action with concrete. All the advantages of massive timber constructions are conserved such as fire resistance. Moreover, concrete with its self-weight improves thermal inertia, acoustical insulation and gives a greater stiffness to the system. It also protects wooden parts from water damages caused by either plumbing problems or fire extinguishing.

The timber-concrete composite structure shown in this paper is drastically improving the stiffness of floors and is in accordance with the latest requirements for modern conveniences housing. As proposed in this paper, this system can be used in a broad variety of constructions, including bridges and factory buildings with the same philosophy of using timber materials at its best, with other complementary structural components.

5. References

- Hoeft, M. 1994. Zur Berechnung von Verbundträgern mit beliebig gefügtem Querschnitt, Thèse No 1213, Ecole Polytechnique Fédéral de Lausanne.
- Götz, K.-H.; Hoor, D.; Möhler, K.; Natterer, J. 1978. Holzbau Atlas, Institut für internationale Architektur-Dokumentation GmbH, München.
- Götz, K.-H.; Hoor, D.; Möhler, K.; Natterer, J. 1989. Timber Design and Construction Sourcebook, McGraw-Hill, Inc.
- Natterer, J.; Herzog, T.; Volz, M. 1991. Holzbau Atlas Zwei, Institut für internattionale Architektur-Dokumentation GmbH, München.
- Natterer, J.; Hoeft, M. 1994. Zum Tragverhalten von Holz-Beton Verbundkonstruktionen Forschungsbericht CERS Nr. 1345, Ecole Polytechnique Fédéral de Lausanne.
- Natterer, J.; Pflug, D.; Hamm, J. 1996 (à paraître). Méthode simplifiée de dimensionnement des dalles mixtes bois-béton, Ecole Polytechnique Fédéral de Lausanne.

Anchoring Stresses between Concrete and Carbon Fibre Reinforced Laminates

Kris BROSENS
Civil Engineer
K.U. Leuven
Heverlee, Belgium

Dionys VAN GEMERT
Professor
K.U. Leuven
Heverlee, Belgium

Summary

When using carbon fibre reinforced laminates for concrete strengthening, the anchoring stresses in the end zones cause special problems. A special shear test specimen is used to study the shear stress distribution and the fracture behaviour in displacement controlled tensile tests. The fracture energy and the bond strength are calculated using fracture mechanics. This paper presents the results of these experiments, and compares the bond strengths predicted by non-linear fracture mechanics and by the actually applied phenomenological design methods.

1. Carbon Fibre Reinforced Plastic (CFRP)

The evolution in the technology of new materials makes it possible to replace the classical steel plates for concrete strengthening by new high-grade materials. This has led to the idea of replacing the steel plates by fibre reinforced composite sheets made of unidirectional, continuous fibres such as glass, carbon and polymers, bonded together with a matrix such as epoxy resin [1,2]. Carbon fibre reinforced epoxy laminates are the most appropriate for strengthening concrete beams. In the early stage these laminates had to be autoclaved, which was difficult to execute in practice. Since the availability of so-called prepreg laminates, these difficulties have disappeared. Prepreg epoxy laminates are preimpregnated with an epoxy resin, which holds the fibres together. The prepreg sheets are very flexible and can be cut easily by means of scissors. At application, the prepreg sheets are impregnated again with the right mixing ratio of epoxy resin components and the chemical reaction is started. When the first layer has hardened enough, the second layer can be applied in the same manner. Several layers, up to 10, can be applied. These prepreg sheets are first developed and produced in Japan. Recently, new UD laminates, which are not preimpregnated, are available. In Belgium the first application of CFRP-laminates took place at the beginning of 1996 [3,4].

2. CFRP laminates versus steel plates

The CFRP laminates have a lot of advantages to classical steel plates. The mechanical properties are superior (table 1).

Properties	CFRP HS	CFRP HM	Steel
Characteristic tensile strength (N/mm ²)	2500	2000	360
Young's Modulus (N/mm ²)	240000	650000	210000
Fibre Cross-section (cm ² /m)	1.67	0.95	---
Fibre Areal weight (g/m ²)	300	200	---
Width of sheet (cm)	25/33	25/33	---
Length of sheet (m)	100	25	6

Table 1 Typical properties of CFRP-sheets and steel plates

The tensile strength of the prepreg sheets is 5 to 10 times higher than that of steel, whereas the modulus of elasticity is comparable to the modulus of steel. Some carbon fibre laminates reach a modulus of elasticity up to 650000 MPa. These good mechanical characteristics allow a smaller cross-section of external reinforcement. Prepreg and UD sheets are also easier to process. Since the CFRP laminates are much lighter - the density is about 3 times lower than the density of steel - the sheets can be placed with less manpower. The CFRP sheets are available on roll, which means that they are available in any length, whereas the steel plates are limited in practice to 6 metre.

Carbon fibres are very corrosion resistant. An expensive surface treatment, like for steel, is not necessary. The CFRP laminates are extremely useful in very corrosive environments, such as marine and chemical aggressive atmospheres. There are some disadvantages too. First it is a brittle material. The carbon fibre behaves linear elastic till rupture, without a plastic phase. The rupture occurs without preceding plastic deformation. The anchorage can give problems too. Due to the high stresses, the CFRP-laminates will peel off easily. The carbon fibres are all oriented longitudinally and the good mechanical properties are only valid in that direction. Without special precautions it is for example impossible to drill a hole, needed for the placement of a dowel. The fibres would be cut and would no longer be able to transfer forces. And finally the price of CFRP-laminates is rather high. The material is much more expensive than steel but the processing cost is much lower. To calculate the total project cost using CFRP laminates all the above elements have to be taken into account.

3. Anchorage of CFRP-laminates

Because of the higher stresses in the CFRP-laminates, the stresses and stress concentrations in the anchorage zone will increase too. Without any precaution the CFRP-laminate might peel off. Extrapolation of the experimental results on the anchorage of steel plates is not allowed. Research concerning the anchoring phenomena has been started at the Reyntjens Laboratory. This investigation deals with the stress distribution and force transfer at the ends of the laminates using non-linear fracture mechanics. The aim is to obtain design rules, based on theoretical and experimental results, to make a safe and economical design possible. Preliminary shear experiments have been done at the Reyntjens Laboratory [5]. Two concrete

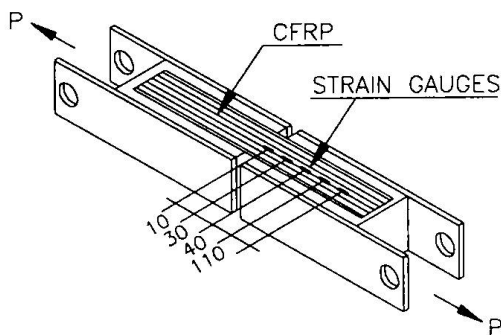


Fig. 1 Test specimen

prisms (150 mm x 150 mm x 300 mm) are connected by gluing 3 layers of CFRP laminates at two opposite sides (figure 1). On the other sides steel plates are glued to apply the tensile force. The test specimen is loaded in a displacement controlled tension machine. Two cardan transmissions assure that the tensile forces act centrically.

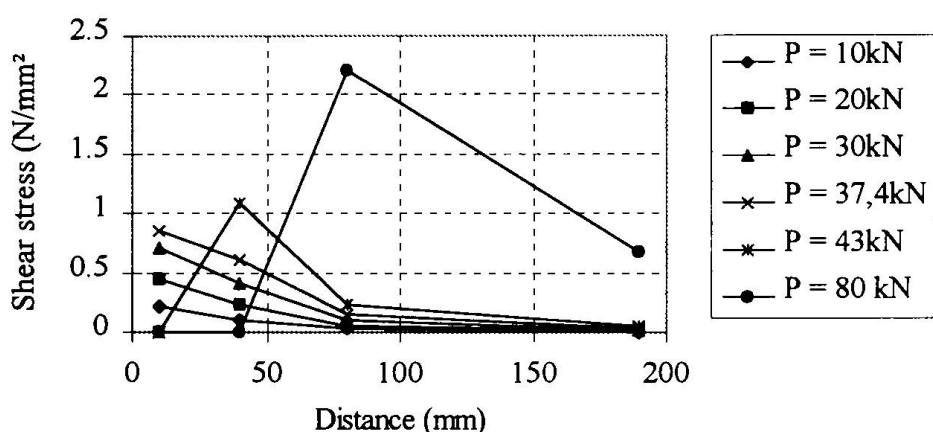


Fig. 2 Shear stresses of specimen A6 (100mm x 200mm)

The load, the deformation of the gap between the two prisms and the strains of the CFRP laminates are recorded during testing. The deformations of the gap are registered with two LVDT-transducers placed at two opposite edges. The strains are measured with strain gauges glued on the CFRP-sheets.

Two series of test specimens, A and B, were manufactured. The compressive strength were respectively 47.9 N/mm² and 46.0 N/mm².

The results show that at the end of the CFRP-sheet a shear stress peak occurs at low forces. When a maximum shear stress is reached the concrete starts to crack. At increasing load, the shear stress peak occur further away from the end zone and the maximum shear stress attains higher values (figure 2). This behaviour seems to be the same as for externally bonded steel plates. The fracture load was compared with the fracture load calculated with the method of Van Gemert [6,7], and with the theory proposed by Täljsten [8] (table 2).

Test Specimen	Bond Length (mm)	Measured fracture load P(kN)	Theoretical fracture load		Difference	
			Täljsten P (kN)	Van Gemert P (kN)	Täljsten (%)	Van Gemert (%)
A1	175	38.7	37.7	18.9	2.6	51.2
A2	150	36.2	31.3	16.2	13.5	55.2
A3	225	41.2	36.2	24.3	12.1	41.0
A4	200	32.1	30.9	21.3	3.7	33.6
A5	200	48.5	43.9	27.0	9.5	44.3
B1	200	55.1	44.1	30.0	20.0	45.6
B2	250	50.8	43.7	37.5	14.0	26.2
B3	250	46.1	35.6	30.0	22.8	34.9
B4	250	34.0	27.6	28.3	18.8	16.8
B5	200	42.4	39.0	24.0	8.0	43.4

Table 2 Test results

The theory used by Täljsten is based on a non-linear fracture energy concept. Steel plates to concrete connections were tested in pure shear, i.e. mode II failure. Both symmetrical and non-symmetrical overlap-joints were considered. When a brittle adhesive ($G > 1.0$ Gpa), such as most epoxy adhesives, is used, the NLFM theory leads to the following expression:

$$P_{\max} = b \sqrt{\frac{2 E_{CFRP} t_{CFRP} G_f}{1 + \alpha}}$$

$$\alpha = \frac{E_{CFRP} t_{CFRP}}{E_{concrete} t_{concrete}}$$

with
 E modulus of elasticity (N/mm²)
 t thickness (mm)
 G_f fracture energy (Nmm/mm²)
 b width of CFRP laminate (mm)

The difficulties of this method are the exact definition of "the fracture energy" and how to calculate this fracture energy from the measured values of the load, deformation and shear stresses. This method can not be used as a design rule. For that purpose a relation between the concrete properties, which can be easily determined, and the fracture energy is needed. Research should be done in that area, especially concerning the fracture energy in glued connections between concrete and other materials, like steel or CFRP-sheets.

The method of Van Gemert is a design rule. The only parameter needed is the tensile strength at the concrete surface, which can easily be measured by means of the pull-off test.

The fracture load found in this way gives the load at cracking of the concrete in the initial force

transfer zone. It does not take into account the reserve available after first cracking. This explains the differences with the experiments. A triangular shear stress distribution is assumed on the basis of a large number of experiments (figure 3). With this assumption an anchorage length is calculated. A large safety factor is used to apply this method for design cases.

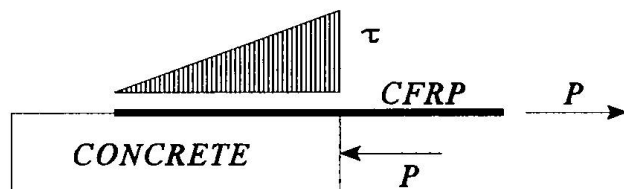


Fig. 3 Shear stress distribution (Van Gemert)

$$P_{\max} = \frac{b l f_{ctk,s}}{2}$$

with b width (N/mm²)
 l bonding length (mm)
 $f_{ctk,s}$ pull-off strength of concrete surface (N/mm²)

The bonded length of the CFRP-sheets on the test prisms were varied too. The fracture load increases when the bonded length increases (figure 4).

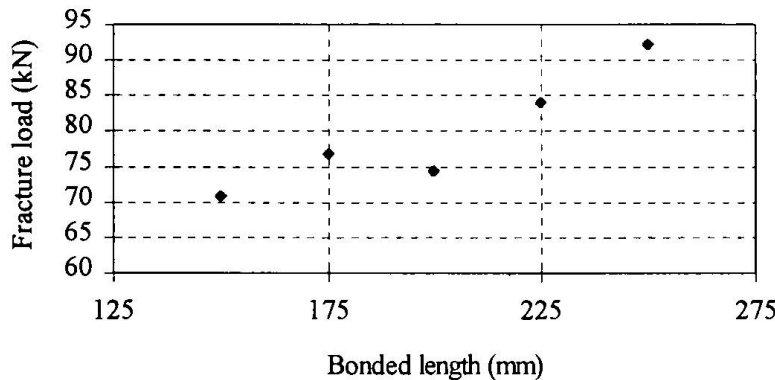


Fig. 4 Influence of bonded length to fracture load (width 80 mm)

However the influence of the bonded length will decrease at larger lengths. Before cracking, the shear stresses reach a maximum value at the end of the CFRP-sheet (figure 5). When the shear stress exceeds the pull-off strength of the concrete surface, the concrete starts to crack [6]. At higher loads, the maximum shear stress shifts to the right (figure 5) and attains higher values. When the direct tensile strength, which is larger than the pull-off strength, is reached, the crack will extend and the sheet will peel off in a brittle way.

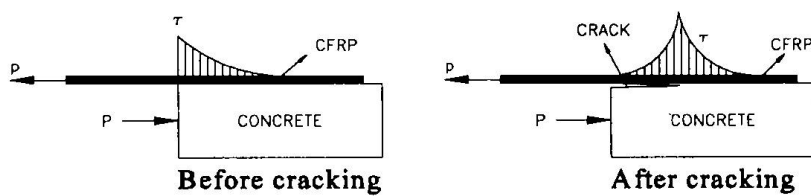


Fig. 5 Shear stress distribution before and after cracking

Once the tensile force from the CFRP-sheet is transferred into the concrete, there are nearly no shear stresses between the remaining sheet and the concrete. This means that when the bonded length exceeds a critical length, the fracture load remains constant. The determination of this critical length can be done experimentally.

In figure 4, the fracture load has not yet attained a constant value, which means that the critical bonded length is at least larger than 275 mm.

4. Conclusions

The use of carbon fibre reinforced materials offers great opportunities in concrete strengthening. A lot of research has to be done to really understand the behaviour in the concrete-CFRP connection. The end zones are the most critical points. Because of the higher stresses in the CFRP laminates, the risk of peeling off increases. Experiments show that the behaviour of externally bonded CFRP-laminates is similar to externally bonded steel plates. A non linear fracture mechanics based design is possible, if the fracture energy G_f of the bonded connection is known. Actually G_f must be determined experimentally, but further research should allow to calculate G_f from the characteristics of the connection and its constituents.

5. Bibliography

- [1] Replark System, Design Guideline, Mitsubishi Chemical Corporation, 1995
- [2] Forca Tow Sheet, Technical Notes, Tonen Corporation, 1995
- [3] Brosens K., Van Gemert D., Vandewalle L., Carbon fibre epoxy laminates for strengthening concrete elements, De Bouwkroniek, 9 februari 1996, pp. 28-32 (in Dutch)
- [4] Van Gemert D., Brosens K., Concrete strengthening with externally bonded plates, CFRP-laminates versus steel plates, Het ingenieursblad (KVIV), jaargang 65, nr. 6-7, juni-juli 1996, pp. 31-36 (in Dutch)
- [5] Van den Heede S., Van Ginderachter K., Anchoring of bonded CFRP reinforcement. Energy measurements at mode II-shearing crack, KULeuven, 1996 (in Dutch)
- [6] Van Gemert D., Vanden Bosch M., Ladang C., Design method for strengthening reinforced concrete beams and plates, second edition, KULeuven, Internal paper 32-ST-17, 1990
- [7] Van Gemert D., Force transfer in epoxy bonded steel-concrete joints, Int. Journal of Adhesion and Adhesive, 1980, nr. 2, pp. 67-72
- [8] Täljsten B., Plate Bonding. Strengthening of existing concrete structures with epoxy bonded plates of steel or fibre reinforced plastics, Doctoral Thesis, Luleå university of technology, Sweden, 1994